Comprehensive analysis of various strategies to improve the diagnostic performance of LR-5 observations in the Liver Imaging Reporting and Data System (LI-RADS) version 2018

Jae Hyon Park

Department of Medicine

The Graduate School, Yonsei University

Comprehensive analysis of various strategies to improve the diagnostic performance of LR-5 observations in the Liver Imaging Reporting and Data System (LI-RADS) version 2018

Jae Hyon Park

Department of Medicine

The Graduate School, Yonsei University

Comprehensive analysis of various strategies to improve the diagnostic performance of LR-5 observations in the Liver Imaging Reporting and Data System (LI-RADS) version 2018

Directed by Professor Yong Eun Chung

Doctoral Dissertation
submitted to the Department of Medicine
the Graduate School of Yonsei University
in partial fulfillment of the requirements for the degree
of Doctor of Philosophy

Jae Hyon Park

June 2021

This certifies that the Doctoral Dissertation
of Jae Hyon Park is approved.

Thesis Supervisor : Yong Eun Chung

Thesis Committee Member#1 : Dong Jin Joo

Thesis Committee Member#2 : Jun Yong Park

Thesis Committee Member#3: Je Sung You

Thesis Committee Member#4: Woo Kyoung Jeong

The Graduate School
Yonsei University

June 2021

ACKNOWLEDGEMENTS

The final outcome of this study required much guidance, support and inspiration from my supervisor, Professor Yong Eun Chung, who is not only my academic mentor in the field of radiology but is also my life mentor. Without his encouragement, guidance, and support, I would not have been able to pursue this theme and I owe to my supervisor the privilege of being his graduate student. I have learned so much from analyzing images to performing complex statistical analyses and I thank Professor Chung for his advice and support throughout my residency..

I would also like to express my deepest gratitude to Professor Dong Jin Joo, Professor Jun Yong Park, Professor Je Sung You, and Professor Woo Kyoung Jeong for their constructive advice and encouragement in finishing my degree and thesis.

In addition, I'd like to extend my thanks to all of my professors in the Department of Radiology at Severance Hospital and National Health Insurance Service (NHIS) Ilsan Hospital for their teachings and for helping me love radiology as a field. I'd like to specially thank Professor Hyung Jin Rhee for all the encouragement and constructive advice he has given me regarding my career and life plan in general and likewise to Professor Nieun Seo for her teachings and guidance in writing a research paper.

Lastly, I'd like to extend my special thanks to my family, my father, mother and my wife-to-be, Insun Park for their spiritual support, love and encouragement in my life.

<TABLE OF CONTENTS>

LIST OF FIGURES

LIST OF TABLES

ABSTRACT

Comprehensive analysis of various strategies to improve the diagnostic performance of LR-5 observations in the Liver Imaging Reporting and Data System (LI-RADS) version 2018

Jae Hyon Park

Department of Medicine
The Graduate School, Yonsei University

(Directed by Professor Yong Eun Chung)

The Liver Imaging Reporting Data System (LI-RADS) is widely adopted for the non-invasive diagnosis of hepatocellular carcinoma (HCC). In this study, the following objectives were investigated: (1) possible strategies to improve the diagnostic performance of LR-5 observations without reducing specificity for HCC were investigated, (2) whether threshold growth is suitable as a major criterion for HCC diagnosis and (3) whether hepatobiliary phase signal intensity can be used to difference HCC with atypical imaging features from non-HCC malignancies within LR-M observations. Herein, treatment naïve patients who underwent gadoxetate-disodium enhanced magnetic resonance imaging and surgical resection for focal hepatic observation were retrospectively analyzed.

When evaluating various strategies to improve LR-5 diagnostic performance, hepatic observations were categorized according to the Liver Imaging Reporting Data System (LI-RADS) version 2018 and the final categories were readjusted by upgrading LR-4 to LR-5 using ancillary features, arterial phase hyperenhancement interpreted with

subtraction images, indication of no washout when arterial phase hyperenhancement was absent, extension of washout to the transitional phase, and subthreshold growth as a major feature. Category-readjusted LR-5 after upgrading LR-4 to LR-5 using ancillary features favoring HCC in particular, subthreshold growth as a major feature, extending washout to transitional phase and arterial phase hyperenhancement interpreted using subtraction images showed significantly increased sensitivity (P<0.001) without decreased specificity (Ps>0.05).

When investigating whether threshold growth should remain as a major feature in the diagnosis of HCC, frequency of the major and ancillary features outlined in the Liver Imaging Reporting Data System (LI-RADS) were evaluated in HCC and non-HCC malignancies. Ancillary feature showing significantly higher prevalence in HCC was used to replace threshold growth as a major feature or was added as an additional major feature and the diagnostic performance of readjusted LR-category was compared to that based on the Liver Imaging Reporting Data System (LI-RADS) version 2018. Unlike APHE, washout, or enhancing capsule which were more frequent in HCCs than non-HCC malignancies, threshold growth was more frequent in non-HCC malignancies than HCCs (P<0.001). The mean size of non-HCC malignancies showing threshold growth was smaller than those without threshold growth (22.2mm vs. 42.9mm, P=0.040) and similarly for HCCs but without significant difference (26.8mm vs. 33.1mm, P=0.184). Fat-in-nodule was more frequent in HCCs than non-HCC malignancies (P=0.027). When fat-in-nodule replaced threshold growth as major feature, LR-5 sensitivity and specificity increased nonsignificantly from 73.2% to 73.9% (P=0.289) and from 98.2% to 98.5% (P>0.999), respectively.

When evaluating whether hepatobiliary phase signal intensity of the tumor can be used to difference HCC with atypical imaging features from non-HCC malignancies, the hepatobiliary phase signal intensity of LR-M observation was categorized into dark, low, and iso-to-high groups. Signal intensity of the tumor was classified as dark when more than 50% of tumor showed hypointensity compared to spleen, as low when more than 50% of tumor showed hyperintensity compared to spleen but hypointensity

compared to liver parenchyme, and as iso-to-high if there was even a focal iso-intensity or hyperintensity compared to liver parenchyma. Analysis of clinicopathological factors and association between imaging and histology was performed. Out of 106 LR-M, 42 (42%) were showed dark, 61 (58%) showed low, and 3 (3%) showed iso-to-high SI in HBP. All 3 iso-to-high SI LR-M were HCCs (P=0.060) and their major histologic differentiation was Edmondson grade 1 (P=0.001). 43 out of 61 (71%) low SI LR-M were iCCA or cHCC-CCA (P=0.002). Inter-reader agreement of HBP SI classification was excellent, with a kappa coefficient of 0.872.

In conclusion, sensitivity of LR-5 was improved without loss of specificity via category readjustment using AFs favoring HCC in particular, subthreshold growth as a major feature, extending washout to transitional phase and APHE interpreted with subtraction images. In addition, threshold growth was found nondiagnostic of HCC and was more common in non-HCC malignancies. Based on our results, comparable diagnostic performance of LR-5 can be obtained if threshold growth is replaced by a more HCC-specific ancillary feature. Lastly, LR-M with iso-to-high signal intensity in hepatobiliary phase was prone to being HCC while LR-M with low signal intensity in hepatobiliary phase was prone to being tumor with fibrous stroma such as iCCA and cHCC-CCA. Classification of LR-M based on hepatobiliary phase signal intensity may serve as a promising method of differentiating HCC with atypical imaging features from non-HCC malignancies.

Key words : liver neoplasm, magnetic resonance imaging, liver, diagnosis, differential

Comprehensive analysis of various strategies to improve the diagnostic performance of LR-5 observations in the Liver Imaging Reporting and Data System (LI-RADS) version 2018

Jae Hyon Park

Department of Medicine
The Graduate School, Yonsei University

(Directed by Professor Yong Eun Chung)

I. INTRODUCTION

Hepatocellular carcinoma (HCC) is one of very few malignancies that can be diagnosed noninvasively without biopsy in patients with cirrhosis or chronic liver disease, largely due to its unique vascular pattern of arterial hyperenhancement followed by washout [1]. Current clinical guidelines suggest that a hepatic observation larger than 1cm can be diagnosed as HCC with high specificity using either dynamic computed tomography (CT) or magnetic resonance imaging (MRI) in high risk patients [1,2] but until the Liver Imaging Reporting and Data System (LI-RADS) was first released in 2011 by the American College of Radiology, considerable variations in image interpretation and reporting impeded the correct diagnosis of HCC[3].

Nowadays, LI-RADS is widely accepted as a good scheme for interpreting and reporting imaging features of hepatic observations on dynamic CT and MRI in patients at high risk of HCC, with hepatic lesion being categorized from LR-1 (definitely benign) to LR-5 (definitely HCC) [4-6]. LI-RADS version 2018 (v2018) [7] is the fourth update of this system, and important changes have been made compared to LI-RADS version 2017 (v2017) [7] to achieve simplicity and consistency with the American Association for the Study of Liver Disease (AASLD) 2018 clinical practice guidance for HCC [8] and the Organ Procurement and Transplantation Network (OPTN) classification system [7,9]. In a subsequent study, however, LR-5 observations according

to LI-RADS v2018 [7] showed increased sensitivity (81% vs. 68%) but reduced specificity (94% vs. 99%) for HCC [6] compared to LR-5 observations according to LI-RADS v2017. In addition, while improved, some elements of the diagnostic algorithm in LI-RADS v2018 remain controversial and in need of validation. Several issues requiring validation include whether the diagnostic performance of LR-5 for HCC can be improved when LR-4 is upgraded to LR-5 using ancillary feature (AF), interpreting nonrim-arterial phase hyperenhancement (APHE) in arterial subtraction images, extending washout to transitional phase, considering no washout when APHE is absent and interpreting subthreshold growth as a major feature. As for ancillary features, LI-RADS v2018 currently does not allow upgrades from LR-4 to LR-5 on the grounds that these features are not specific for HCC and may lower LR-5 specificity for HCC, but a recently independently significant AF was found to increase sensitivity of LR-5 without impairing specificity on gadoxetic acid enhanced MRI [10].

In addition, since the first LI-RADS v2014, five major features including arterial phase hyperenhancement (APHE), washout, enhancing capsule, diameter, and threshold growth, have been established as major features to arrive at an initial category which is later adjusted using ancillary features. Among major features, APHE has consistently shown high sensitivity for progressed HCC as it reflects increased intranodular arterial supply during hepatocarcinogenesis [11-13]. Likewise, washout is also considered a strong predictor of HCC as it reflects the decreased portal supply accompanied by the progression of the histologic grade of the tumor [13,14]. Combined together, these two features show a high specificity for HCC in patients with cirrhosis or other risk factors of HCC [15,16]. In addition, enhancing capsule, while less sensitive, is also reported to not only be specific for HCC but also directly correlates with either the tumor capsule in progressed HCC or pseudocapsule consisting of mixed fibrous tissue and dilated sinusoids [17,18].

These three major features have strong pathophysiologic basis in the hepatocarcinogenesis of HCC, are well-established in the context of HCC diagnosis, and included in all major imaging based HCC diagnostic algorithms [8,19-21]. In contrast,

the latest LI-RADS version 2018 (v2018) limits the definition of threshold growth to "≥50% increase in diameter in ≤6 months" which is arbitrary, dictated by a need for congruence to the OPTN algorithm [9], and based mainly on expert opinion. In addition, although interval growth is an important feature for radiologists to consider in the diagnosis of any neoplasm, the growth rate of HCC can vary widely owing to its initial tumor size or histologic differentiation of the lesion [22-24]. Furthermore, while threshold growth may be useful in reducing the false-positive diagnosis by differentiating slow-growing benign entities, it has limited value in differentiating growing hepatic malignancies including intrahepatic mass-forming cholangiocarcinoma (iCCA) or combined HCC-cholangiocarcinoma (cHCC-CCA), which can also occur in HCC high-risk patients. In fact, the reported tumor doubling times of HCC [22,23] overlap significantly with that of iCCA [25]. In a previous study, removal of threshold growth from major features was found to cause significant proportion, about 9%, of LR-5 observations to downgrade to LR-4 [26] but no study has yet evaluated whether replacing threshold growth with an ancillary feature will cause similar impact on the LI-RADS categorization.

Moreover, LI-RADS v2018 includes a special category, LR-M, for observations that are probably or definitely malignant but not necessarily hepatocellular carcinoma (HCC) [7]. The aim of this category, when first introduced, was to maintain the specificity of LR-5 (definitely HCC) without losing the sensitivity to detect malignancies including HCC with atypical imaging features, intrahepatic mass forming cholangiocarcinoma (iCCA) and combined hepatocellular cholangiocarcinoma (cHCC-CCA) [7,27]. Although new explicit LR-M criteria have been introduced through LI-RADS v2017 (same in v2018) including targetoid apperance and several nontargetoid imaging features, the diagnostic performance of LR-M for non-HCC malignancy has been variable [5,28,29]. Not only does the ambiguous criteria of LR-M makes it susceptible to the subjectivity of each radiologist but also the heterogeneous group of disease entities given this category makes it difficult for accurate imaging prediction of the likely etiology of LR-M observation [30].

However, differential diagnosis of HCC from non-HCC malignancies on imaging is critical because pathologic confirmation is not always mandated before instituting treatment in case of HCC and also because HCC differs from non-HCC malignancies such as cHCC-CCA and iCCA with regard to possible candidacy for liver transplantation and prediction of prognosis [31,32]. In such case, it would be important to accurately categorize LR-M HCCs with atypical imaging features as definitely HCC in patients with Barcelona Clinic Liver Cancer (BCLC) stage 0/A and Child Pugh class A who are eligible and can benefit curative treatment from liver transplantation [33-35]. Likewise, a more accurate image prediction of non-HCC malignancy within LR-M observations by differentiating non-HCC malignancies from HCC with atypical imaging features may help narrow patients in need and urgency of biopsy. Either way, a more accurate diagnosis of HCC or non-HCC malignancy among LR-M in patients of high risk of HCC hold mutual clinical significance for both groups. In addition, most of the previous studies [36-38] regarding LR-M observations have focused on imaging findings that can differentiate iCCA or cHCC-CCA from HCC among LR-M observations.

LI-RADS v2018 states that at least one imaging feature suggestive of hepatocellular origin represents HCC with atypical feature or cHCC-CCA, one of which consists of hepatobiliary phase (HBP) hyperintensity greater than signal intensity of surrounding liver [7]. On the other hand, it also states that targetoid appearance represents iCCA or cHCC-CCA and even few HCC with atypical features, but targetoid appearance in hepatobiliary phase, which is characterized by a moderate to marked hypointensity in periphery with milder hypointensity in center, is close to the phenomenon referred to as “gadoxetic acid cloud” often noted in iCCA, previously suggested to be due to intratumoral fibrous stroma[39]. Thus, categorization based on tumoral signal intensity in HBP may possibly be a useful in categorizing LR-M observations.

Thus, the purpose of this study was to explore possible strategies of improving the diagnostic performance of LR-5 for HCC by (1) adjusting the final LR-category by upgrading LR-4 to LR-5 using ancillary feature (AF), interpreting nonrim-arterial phase

hyperenhancement (APHE) in arterial subtraction images, extending washout to transitional phase, considering no washout when APHE is absent, and considering subthreshold growth as a major feature; (2) investigating whether threshold growth should remain as a major feature and calculating the diagnostic performance of LR-5 when threshold growth is replaced by a more HCC-specific feature; and (3) evaluating whether tumor signal intensity in hepatobiliary phase can be used to differentiate HCC with atypical imaging features from non-HCC malignancies among LR-M observations. In case of (3), image-histologic correlation was performed to provide histopathologic basis for the image manifestation and provide rationale to our criteria.

II. MATERIALS AND METHODS

1. Diagnostic performance of category adjusted LR-5 using modified criteria

A. Study population

This Health Insurance Portability and Accountability Act-compliant (HIPAA) study was approved by our institutional review board of Yonsei University College of Medicine and written informed consent was waived due to its retrospective study design. Using electronic medical records, patients with cirrhosis or chronic hepatitis B virus infection who underwent gadoxetate disodium-enhanced MRI between January 2009 and December 2014 for the evaluation of focal hepatic lesions were identified. Herein, a hepatic observation was defined as any area distinct from the background liver detected on any phase of routine MRI sequences [7]. Inclusion criteria were patients who (1) underwent liver surgery within 6 months from the date of the MRI exam, (2) had no history of treatment for hepatic observations before the MRI exam and (3) were pathologically diagnosed such as through surgical resection. On the other hand, patients who (1) had underlying congestive hepatopathy or iron-deposition liver disease including hemochromatosis or Wilson's disease, (2) had >3 hepatic observations and (3) did not have all the required images of the MRI protocol were excluded from analysis. For patients with more than one but <3 hepatic observations, the largest observation with a corresponding histopathologic diagnosis was analyzed.

B. MRI acquisition

All patients underwent MRI examinations on a 3.0- MRI unit. Dynamic MRI studies of the liver were performed after 10 mL of gadoxetate disodium (Primovist; Bayer AG, Berlin, Germany) was injected followed by 20 mL of 0.9% saline at injection rate of 1 mL/s. T1-weighted 3D gradient-echo imaging was obtained before contrast injection. Arterial phase imaging was initiated using either a test bolus technique with 1mL of gadoxetic acid or the bolus-tracking technique, and images from the portal venous phase, transitional phase, and hepatobiliary phase were obtained at approximately 60, 90, and 150 seconds and 20 minutes after the administration of the contrast agent began, respectively. Subtraction images were automatically generated after image acquisition on the MRI console that provided image-by-image subtractions or were manually generated by AquariusNET (Tera-Recon, San Mateo, CA, USA) between the unenhanced and arterial phases of each patient.

Other MRI sequences included an axial dual-echo T1-weighted breath-hold gradient echo sequence for acquisition of in-phase and out-of-phase images, an axial respiratory-triggered turbo spin-echo T2-weighted sequence with fat saturation, an axial half-Fourier acquisition single-shot turbo spin-echo T2-weighted sequence with fat saturation, and diffusion-weighted imaging with respiratory-triggered single-shot echo planar imaging sequences with *b* values of 0, 50, 400 and 800 sec/mm^2 or 50, 400 and 800 sec/mm^2.

C. MR Image analysis and LI-RADS category assignment

One board-certified radiologist with 11 years (Y.E.C) of experience with liver MRI and a senior radiology resident (J.H.P) retrospectively reviewed and analyzed the images together. Prior to image analysis, senior radiology resident (J.H.P) selected a lesion (the largest lesion, if multiple lesions in a patient had received histopathologic diagnoses) corresponding to the pathology report findings. All MRIs were reviewed via a picture archiving and communication system (PACS) (Centricity Radiology RA 1000;

GE Healthcare, Chicago, IL, USA). While both readers were aware that all patients had undergone MRI because of suspected focal hepatic lesions and that the patients either had liver cirrhosis or chronic hepatitis B viral infection, the readers were blinded to the histopathological results.

Lesion size, location, major features, targetoid mass features and AFs as well as the final LR-category of the hepatic observations were evaluated according to LI-RADS v2018 [7]. Presence of APHE was examined in both the ordinary late arterial phase image and arterial subtraction image. A minimum interval of two weeks had to pass before the arterial subtraction images were analyzed to avoid possible recall bias.

D. Validation study of the diagnostic performances of different category-adjusted LR-5 for HCC

Diagnostic performances of different category-adjusted LR-5 for HCC were compared to the diagnostic performance of the original LR-5. Categories were readjusted under six different conditions: 1) using AFs favoring malignancy in general including AFs favoring HCC in particular (any one of subthreshold growth, restricted diffusion, mild-moderate T2 hyperintensity, corona enhancement, fat sparing in solid mass, iron sparing in solid mass, transitional phase hypointensity and hepatobiliary phase hypointensity, nonenhancing capsule, nodule-in-nodule, mosaic architecture, blood products in mass, fat in mass more than adjacent liver) to upgrade LR-4 to LR-5; 2) using AFs favoring HCC in particular (any one of nonenhancing capsule, nodule-in-nodule, mosaic architecture, blood products in mass, fat in mass more than adjacent liver) to upgrade LR-4 to LR-5. For conditions 1) and 2), categories were adjusted in the presence of $\geq$1 AF favoring malignancy in general (including AFs favoring HCC in particular) and in the presence of $\geq$1 AF favoring HCC in particular only, respectively, even though upgrade from LR4 to LR5 is prohibited in LIRAD v2018. No category adjustment was made in the presence of $\geq$1 AF favoring benignity which was consistent with the v2018 diagnostic algorthm. In addition, LR-3 lesions that had already been upgraded to LR-4 lesions were not eligible for category adjustment

using AFs; 3) LI-RADS v2018 [7] dictates that nonrim APHE can only be called if the signal intensity of the observation on the arterial phase is unequivocally greater than the liver and states that the subtraction image may be used optionally when evaluating APHE. Under condition 3), APHE is called if hyperintensity is seen in the subtraction image, which is made by the subtraction of pre-contrast image from late arterial phase image; 4) In addition, LI-RADS v2018 [7] defines washout as any temporal reduction in enhancement relative to composite liver tissue in the portal venous phase regardless of the presence of APHE in the late arterial phase. Under condition 4), presence of washout was interpreted only when there was an initial "wash-in" or APHE in the late arterial phase. All other reduced enhancements in the portal venous phase of hepatic observations without APHE in the late arterial phase were not considered as washout; 5) Extending washout to the transitional phase; and 6) Considering subthreshold growth as a major feature rather than AFs favoring malignancy: in previous LI-RADS v2017, threshold growth was defined as one of "≥ 50% size increase within ≤6 months", "≥ 100% size increase within > 6 months" and "new ≥ 10mm nodule within ≤ 24 months" wherein the last two definitions no longer meet criteria for threshold growth and are considered as subthreshold growth in LI-RADS v2018 while the definition of subthreshold growth being "unequivocal size increase of mass, less than threshold growth" remains unchanged in both LI-RADS v2017 and LI-RADS v2018. In this study, the diagnostic performance was evaluated when "≥ 100% size increase within > 6 months" and "new ≥ 10mm nodule within ≤ 24 months" were again considered as threshold growth as in previous LI-RADS v2017 rather than using LI-RADS v2018 definition.

E. Histopathologic diagnosis

Diagnosis of HCC and non-HCC malignancies were confirmed via pathology. Benign diagnoses were obtained through pathology (n=3) or typical imaging features or stability at imaging for at least 2 years (n=226). The fibrosis stage of the liver

parenchyma was assessed according to the Batts-Ludwig scoring system from F0, no fibrosis to F4, cirrhosis [40,41], if available in the pathology report.

F. Statistical analysis

Patient characteristics were compared between the two groups using the X^2-test or the Fisher exact test for categorical variables and the Student *t* test for continuous variables. Since only one lesion was selected for image analysis, the endpoints were analyzed on a per patient basis [5]. Estimates and 95% confidence intervals (CIs) of diagnostic performance including sensitivity, specificity, positive predictive value and negative predictive value were calculated for LR-5 as well as for the combination of LR-4 and LR-5 in LI-RADS v2018. Diagnostic performances of the category-adjusted LR-5 were also calculated and compared to that of the original v2018 LR-5 using McNemar's test. Receiver operating characteristic (ROC) curves were drawn and an area under the curve (AUC) was calculated. Pairwise comparison of ROC curves were done and *P*-values were recorded. A two-sided *P*-value <0.05 was considered to indicate a statistically significant difference. All statistical analyses were performed using MedCalc, version 19.0.7 (MedCalc Software, Ostend, Belgium) and SPSS, version 25 (IBM, Chicago, IL, USA).

2. Threshold growth as a major feature the diagnosis of HCC

A. Study population

Again, this part of the study was approved by the institutional review board of Yonsei University College of Medicine and the requirement for written informed consent was waived due to its retrospective study design. Using electronic medical records, patients with underlying liver cirrhosis or chronic hepatitis B viral infection who underwent gadoxetate disodium enhanced MRI between January 2009 and December 2016 for the evaluation of a focal hepatic observation were identified. Patients who (1) underwent surgical resection within 6 months from the date of MRI exam, (2) had not previously been treated for hepatic observation prior to MRI exam,

(3) and were pathologically diagnosed via surgical specimen were included. Likewise, patient who (1) had underlying congestive hepatopathy or iron-deposition liver disease, (2) had >3 hepatic observations and (3) did not have all required images of MRI protocol were excluded from analysis. For patients with more than one observation, the largest observation and its corresponding histopathologic diagnosis was used for the analysis.

B. MR acquisition

MR imaging techniques for this part of the study were same as that written in (II)-(1)-(B) under MR acquisition for the evaluation of diagnostic performance of category adjusted LR-5 using modified criteria.

C. MR image analysis and LI-RADS category assignment

Again, one board-certified radiologist with 11 years (Y.E.C) of experience with liver MRI and a senior radiology resident (J.H.P) retrospectively reviewed the images. Image analysis was peformed on the largest lesion, if multiple lesions had received histopathologic diagnosis in one patient, after excluding benign observations corresponding to LR-1 and LR-2. All MRIs were retrieved and reviewed via a picture archiving and communication system (PACS) (Centricity Radiology RA 1000; GE Healthcare, Chicago, IL). Reviewers analyzed each hepatic observation according to LI-RADS v2018 [7]. For observations with documented threshold growth, reviewers determined the qualifying threshold growth criteria ($\geq$50% increase in diameter in $\leq$6months) by retrospectively reviewing, measuring and comparing the longest diameter of observation of current and prior exams in either transitional or hepatobiliary phase for liver dynamic MRI and portal venous phase or delayed phase for liver CT.

D. Adjustment of major and ancillary features in LI-RADS v2018

Ancillary features that showed significantly higher frequency in HCC compared to non-HCC under the univariate analysis (i.e. X^2-test or Fisher's exact test) were

considered as possible candidates for new major feature. Final LR-category was then re-evaluated under the conditions that these features replace current major features or are added as additional major features.

E. Histopathologic diagnosis

Final diagnosis of hepatic observation and status of adjacent non-tumor liver parenchyma were extracted from pathology report. For HCC, tumor grade was categorized as I, II, III and IV based on the nuclear grading scheme proposed by Edmondson and Steiner [42]. Benign diagnoses were obtained through pathology (n=3) or typical imaging features or stability at imaging for at least 2 years (n=336) [43]. Fibrosis stage of non-tumor liver parenchyma was assessed according to Batts-Ludwig scoring system from F0, no fibrosis to F4, cirrhosis [40]

F. Statistical analysis

Baseline characteristics of patients were compared using the X^2-test or the Fisher exact test for categorical variables and the Student t test or Wilcoxon signed-rank test for continuous variables. Continuous variables are expressed as median and interquartile range. Imaging feature end points were evaluated on a per patient basis since one hepatic observation in each patient was selected for image analysis [5]. Estimates and 95% confidence intervals (CIs) of diagnostic performance including sensitivity, specificity, positive predictive value, negative predictive value and accuracy were calculated. Then, diagnostic performance of adjusted LR-5 was also calculated and compared to that of original LR-5 using McNemar's test. Fisher's exact test was used to evaluate correlation between threshold growth and Edmondson grade of HCC and Cochran-Armitage's trend test was used to evaluate whether presence of Edmondson grade was higher in presence over abscence of threshold growth. Two sided *P*-value <0.05 was considered as statistically significant. All statistical analyses were performed by using MedCalc, version 19.0.7 (MedCalc Software, Ostend, Belgium) and SPSS, version 25 (IBM, Chicago, IL, USA).

3. Usefulness of hepatobiliary phase signal intensity in the diagnosis of HCC with atypical imaging features among LR-M observations

A. Study population

Again, this part of the study was approved by our institutional review board and the requirement for patient consent was waived due to its retrospective design. Using electronic medical records, patients with underlying liver cirrhosis or chronic hepatitis B-viral infection who underwent gadoxetate-disodium enhanced MRI between January 2009 and December 2018 for the evaluation of a focal hepatic observation were identified. Patients who (1) underwent surgical resection within 6 months from date of MRI exam, (2) had not previously been treated for hepatic observation prior to MRI study, and (3) were pathologically diagnosed via surgery were included. Likewise, patients who (1) had poor MR image quality and (2) did not have all required images of MRI protocol were excluded from analysis. Based on these inclusion and exclusion criteria, 1,286 hepatic observations were eligible for study. The MRI data, surgical notes and pathology reports for the largest observation in these patients were retrospectively reviewed. Two radiologists classified these observations according to LI-RADS v2018 in consensus [7], and tumor-in-vein (LR-TIV) and LR-1 to 5 observations were excluded, leaving 107 LR-M observations. According to LI-RADS v2018, LR-M is assigned to either targetoid mass or nontargetoid mass with one of infiltrative appearance, marked diffusion restriction, necrosis or severe ischemia and other feature that radiologist judges to sugesst non-HCC malignancy [7].

Among 107 LR-M observations, one observation was excluded since hepatobiliary phase signal intensity of the observation could not be compared to the signal intensity of the spleen due to splenectomy status.

Clinical information and laboratory data of final 106 LR-M observations were then retrospectively reviewed and included the following: patient demographics, cause of chronic liver disease, serum levels of aspartate transaminase, alanine transaminase, total bilirubin, albumin, prothrombin time, platelets, α-fetoprotein, protein induced by

vitamin K absence (PIVKA)-II, carbohydrate antigen 19-9 (CA 19-9), and carcinoembryonic antigen (CEA).

B. MR acquisition

MR imaging techniques for this part of the study were same as that written in (II)-(1)-(B) under MR acquisition for the evaluation of diagnostic performance of category adjusted LR-5 using modified criteria.

C. MR image analysis

One board certified radiologist and a senior radiology resident independently reviewed MR images using picture archiving and communication system (PACS) (Centricity Radiology RA 1000; GE Healthcare, Chicago, IL). Both reviewers were blinded to patient's clinical information and tumor histopathologic features. Tumor was classified in the dark group when more than 50% of tumor area showed hypointensity compared to spleen, in the low group when more than 50% of tumor area showed hyperintensity compared to spleen but hypointensity compared to liver parenchyme, and in the iso-to-high group if there was even a focal iso-intensity or hyper-intensity compared to liver parenchyma on visual insepction in hepatobiliary phase image [44]. When equivocal on visual inspection, ROI was drawn on tumor, spleen and liver parenchyme to quantify and compare the signal intensities.

D. Histopathologic diagnosis

Final diagnosis of hepatic observation and status of non-tumor liver parenchyma including presence of cirrhosis were extracted from pathology reports. For HCC, size, architectural pattern, variant/subtype and major histologic differentiation based on the nuclear grading scheme proposed by Edmondson and Steiner [42] were recorded. As for non-HCC malignancies, size and major histologic differentiation (well/moderate/poor/undifferentiated) were recorded. Presence of tumor necrosis (>5%), percentage of tumor necrosis in gross specimen, capsular formation status, and microvascular invasion status were recorded for all tumors.

E. Statistical analysis

Inter-reader agreement was expressed by Cohen's kappa coefficient. A kappa statistic of 0.8-1.0 was considered excellent agreement, 0.6-0.89 good agreement, 0.40-0.59 moderate agreement, 0.2-0.39 fair agreement and 0-0.19 poor agreement. To compare features of HCC and non-HCC malignancies, we used Mann-Whitney U test for continuous variables and the X^2 or Fisher exact test for categorical variables. The association analyses of hepatobiliary phase signal intensity group versus tumor group and histopathologic findings were performed by calculated Pearson's correlation coefficients and *P*-values. Bonferroni correction was used for post hoc multiple comparisons for all statistical analyses. Two-sided *P*-values <0.05 were considered statistically significant. All statistical analyses were performed using R software (version 3.4.0; The R Foundation for Statistical Computing, Vienna, Austria).

III. RESULTS

1. Diagnostic performance of category adjusted LR-5 using modified criteria

A. Patient characteristics and pathologic findings

Based on the inclusion and exclusion criteria, 796 potential eligible patients were identified. After excluding four patients with tumor in a vein, 792 patients were finally included in this study (Figure 1). Clinico-pathologic characteristics of the 792 patients (616 men and 176 women; mean age, 56 years ± 10; range, 28-85 years) are summarized in Table 1. Median size of HCC, non-HCC malignancies and benign lesions were 29.4mm, 36.2mm and 11.0mm, respectively. Out of the total 508 HCCs, 5 were <10mm, 90 were 10-19mm and 413 were ≥20mm in size.

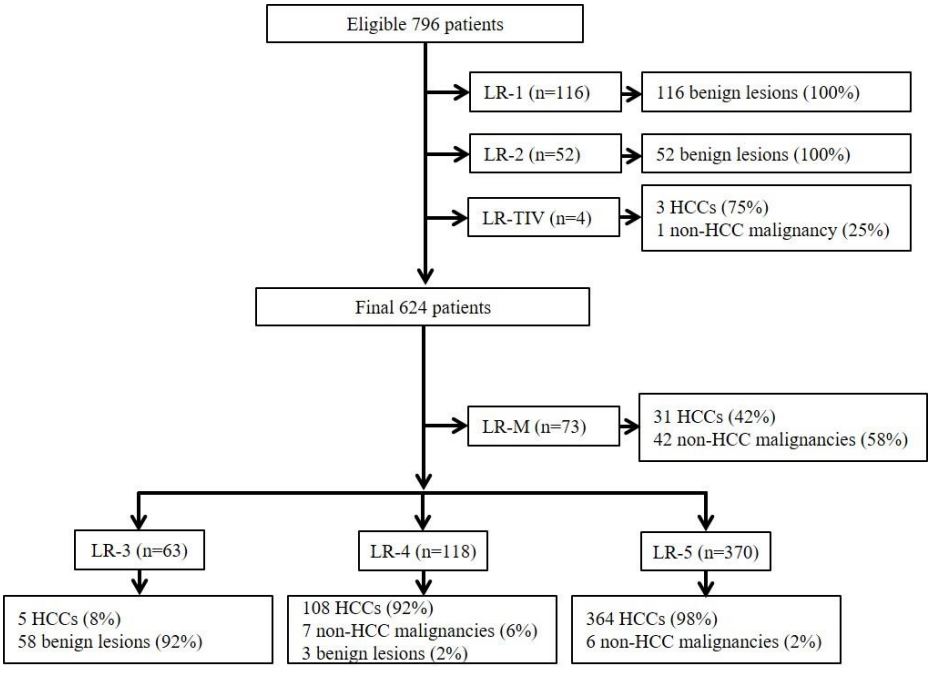

Figure 1. Study flow diagram. HCC, hepatocellular carcinoma

Table 1. Clinical-pathologic characteristics of patients and hepatic observations

Characteristics	Value
Patients (n= 792)	
Mean age (y)*	56.2±10.0
Sex	
Men	616 (77.8)
Women	176 (22.2)
Cause of liver disease	
Hepatitis B virus	650 (82.1)
Alcohol	51 (6.4)
NASH	43 (5.4)
Hepatitis C virus	27 (2.4)
Autoimmune	1 (0.1)
Cryptogenic	20 (2.5)
Number of observations per patient	
1	666 (84.1)
2	65 (8.2)
3	61 (7.7)
Lesions (n=792)	
Median size (mm)**	25.2 (25.0)
HCC	29.4 (20.5)

Non-HCC malignancies	36.2 (26.4)
Benign lesions	11.0 (9.0)
Final diagnosis	
HCC	508 (64.1)
Non-HCC malignancies	55 (6.9)
iCCA	27 (49.1)
cHCC-CCA	23 (41.8)
Metastasis	4 (7.3)
Sarcomatoid cHCC-CCA	1 (1.8)
Benign lesions (n=229)	
Hemangioma	143 (62.4)
Dysplastic or regenerative nodules	46 (20.1)
FNH-like nodule	23 (10.0)
Eosinophilic infiltration	12 (5.2)
Focal fat-deposition	3 (1.3)
Inflammatory pseudotumor	1 (0.4)
Focal fat-sparing	1 (0.4)
Acute and chronic inflammation with granulation tissue and fibrosis	1 (0.4)
Pathologically confirmed liver fibrosis (n=566)	
Cirrhosis (Grade 4)	332 (58.7)
Septal fibrosis (Grade 3)	99 (17.5)
Periportal fibrosis (Grade 2)	80 (14.1)
Portal fibrosis (Grade 1)	55 (9.7)
Median time interval between MRI and pathologic diagnosis (d)**	13 (14)

Note- Unless stated otherwise, data are number of patients or observations. Data in parentheses are percentages.
Abbreviations: cHCC-CCA, combined HCC-choangiocarcinoma; FNH, focal nodular hyperplasia; HCC, hepatocellularcarcinoma; iCCA, intrahepatic mass-forming cholangiocarcinoma; NASH, non-alcoholic steatohepatitis; y, years; d, days
*Data are means ± standard deviations.
**Data are presented as median values. Data in parentheses are interquartile ranges and were calculated as the difference between the 75th and 25th percentiles.

B. Diagnostic performance for HCC using LI-RADS v2018

Based on the diagnostic algorithm of LI-RADS v2018, the final LI-RADS categories of the 792 hepatic observations were as follows: 73 LR-M, 116 LR-1, 52 LR-2, 63 LR-3, 118 LR-4, and 370 LR-5 (Figure 1). Based on these categorizations, LR-5 showed a sensitivity of 71.9% and a specificity of 97.9% for the diagnosis of HCC (Table 2).

Table 2. Sensitivity, specificity, accuracy, positive predictive value (PPV) and negative predictive value (NPV) of hepatocellular carcinoma (HCC) under various categorizations via LI-RADS v2018

	Sensitivity (%)	Specificity (%)	PPV (%)	NPV (%)	Accuracy (%)	*P*-value[a]	*P*-value[b]
LIRADS v2018 LR-4 and 5	92.9 (472/508) [90.3, 95.0]	94.4 (268/284) [91.0, 96.8]	96.7 (472/488) [94.8, 97.9]	88.2 (268/304) [84.4, 91.1]	93.4 (740/792) [91.4, 95.1]	-	-
LIRADS v2018 LR-5	71.9 (365/508) [67.7, 75.7]	97.9 (278/284) [95.5, 99.2]	98.4 (365/371) [96.5, 99.3]	66.0 (278/421) [62.8, 69.1]	81.2 (643/792) [78.3, 83.8]	-	-
Upgraded LR-5 using malignancy AF in general	88.2 (448/508) [85.1, 90.9]	95.1 (270/284) [91.9, 97.3]	97.0 (448/462) [95.1, 98.2]	81.8 (270/330) [78.0, 85.1]	90.7 (718/792) [88.4, 92.6]	<0.001	0.008
Upgraded LR5 using HCC AF	78.9 (401/508) [75.1, 82.4]	97.5 (277/284) [95.0, 99.0]	98.3 (401/408) [96.5, 99.2]	72.1 (277/384) [68.6, 75.4]	85.6 (678/792) [83.0, 88.0]	<0.001	>0.999
LR-5 after extending the evaluation of APHE to the subtraction image**	74.4 (378/508) [70.4, 78.2]	97.9 (278/284) [95.5, 99.2]	98.4 (378/384) [96.6, 99.3]	68.1 (278/408) [64.8, 71.3]	82.8 (656/792) [80.0, 85.4]	<0.001	>0.999
LR-5 when considering no washout if no APHE.	71.3 (362/508) [67.1, 75.2]	97.9 (278/284) [95.5, 99.2]	98.4 (362/368) [96.5, 99.3]	65.6 (278/424) [62.4, 68.6]	80.8 (640/792) [77.9, 83.5]	0.250	>0.999
LR-5 after extending evaluation of washout from PVP to TP.	75.6 (384/508) [71.6, 79.3]	96.8 (275/284) [94.1, 98.5]	97.7 (384/393) [95.7, 98.8]	68.9 (275/399) [65.5, 72.1]	83.2 (659/792) [80.4, 85.8]	<0.001	0.250
LR-5 if not using subthreshold (subthreshold =threshold) [LR v2017 vs.	74.8 (380/508) [70.8, 78.5]	97.9 (278/284) [95.5, 99.2]	98.5 (380/386) [96.6, 99.3]	68.5 (278/406) [65.1, 71.6]	83.1 (658/792) [80.3, 85.6]	<0.001	>0.999

LR v2018]

All diagnostic performances are calculated for HCC.
Abbreviations: AF, ancillary features; APHE, (nonrim) arterial phase enhancement; HCC, hepatocellular carcinoma; LI-RADs, Liver Imaging Reporting and Data Systems; PVP, portal venous phase; TP, transitional phase.
**APHE is evaluated in both the arterial phase image and the subtraction (arterial phase-precontrast phase) image.
Numbers in parentheses are the 95% confidence intervals (CIs).
[a]*P*-value after comparing sensitivity to that of LR-5* using McNemar's test
[b]*P*-value after comparing specificity to that of LR-5* using McNemar's test

C. Diagnostic performance of LR-5 for HCC after category adjustment of LR-4 using AFs

Among a total 118 LR-4 observations, 83 observations (70.3%) were found eligible for upgrade to LR-5 using AFs favoring malignancy in general (including AFs favoring HCC in particular) defined by LI-RADS v2018. This adjusted LR-5 resulted in significantly increased sensitivity (88.2%, $P<0.001$) and decreased specificity (95.1%, $P=0.008$) for HCC (Table 2).

On the contrary, when applying AF favoring HCC in particular only, 36 out of a total 118 LR-4 observations (30.5%) were found eligible for upgrade to LR-5. After category adjustment, LR-5 sensitivity significantly increased (78.9%, $P<0.001$) without decreasing its specificity (97.5%, $P>0.999$) for HCC (Table 2). Comparison of ROCs showed significant increase in AUCs of both LR-5 upgraded with AFs favoring malignancy in general and LR-5 upgraded with AFs favoring HCC in particular ($P<0.001$). (Table 3).

Table 3. Area under the curve (AUC) of various categorizations

	AUC (95% CI)	*P*-value[a]
LIRADS v2018 LR-4 and 5	0.936 [0.917, 0.952]	-
LIRADS v2018 LR-5	0.849 [0.822, 0.873]	-
Upgraded LR-5 using malignancy AF in general	0.916 [0.895, 0.935]	<0.001
Upgraded LR5 using HCC AF	0.886 [0.862, 0.908]	<0.001
LR-5 after extending the evaluation of APHE to the subtraction image**	0.861 [0.835, 0.885]	<0.001
LR-5 when considering no	0.846 [0.819, 0.870]	0.083

washout if no APHE.		
LR-5 after extending evaluation of washout from PVP to TP.	0.862 [0.836, 0.885]	0.010
LR-5 if not using subthreshold (subthreshold=threshold) [LR v2017 vs. LR v2018]	0.863 [0.838, 0.885]	<0.001

Numbers in parentheses are the 95% confidence intervals (CIs).
All diagnostic performances are calculated for HCC.
Abbreviations: AF, ancillary features; APHE, (nonrim) arterial phase enhancement; HCC, hepatocellular carcinoma; LI-RADs, Liver Imaging Reporting and Data Systems; PVP, portal venous phase; TP, transitional phase.
[a]*P*-value of pairwise comparison of ROC curves (compared to LR-5*)

D. Diagnostic performance of LR-5 for HCC after extending APHE to the subtraction image

In the detection of APHE, among 81 HCCs that did not show APHE in late arterial phase, 16 (19.8%) showed APHE in arterial subtraction images. Out of these 16 observations, 13 observations had their final LR categories adjusted from LR-4 to LR-5 when APHE was interpreted using subtraction image. (Figure 2). All 13 observations were later confirmed as HCCs.

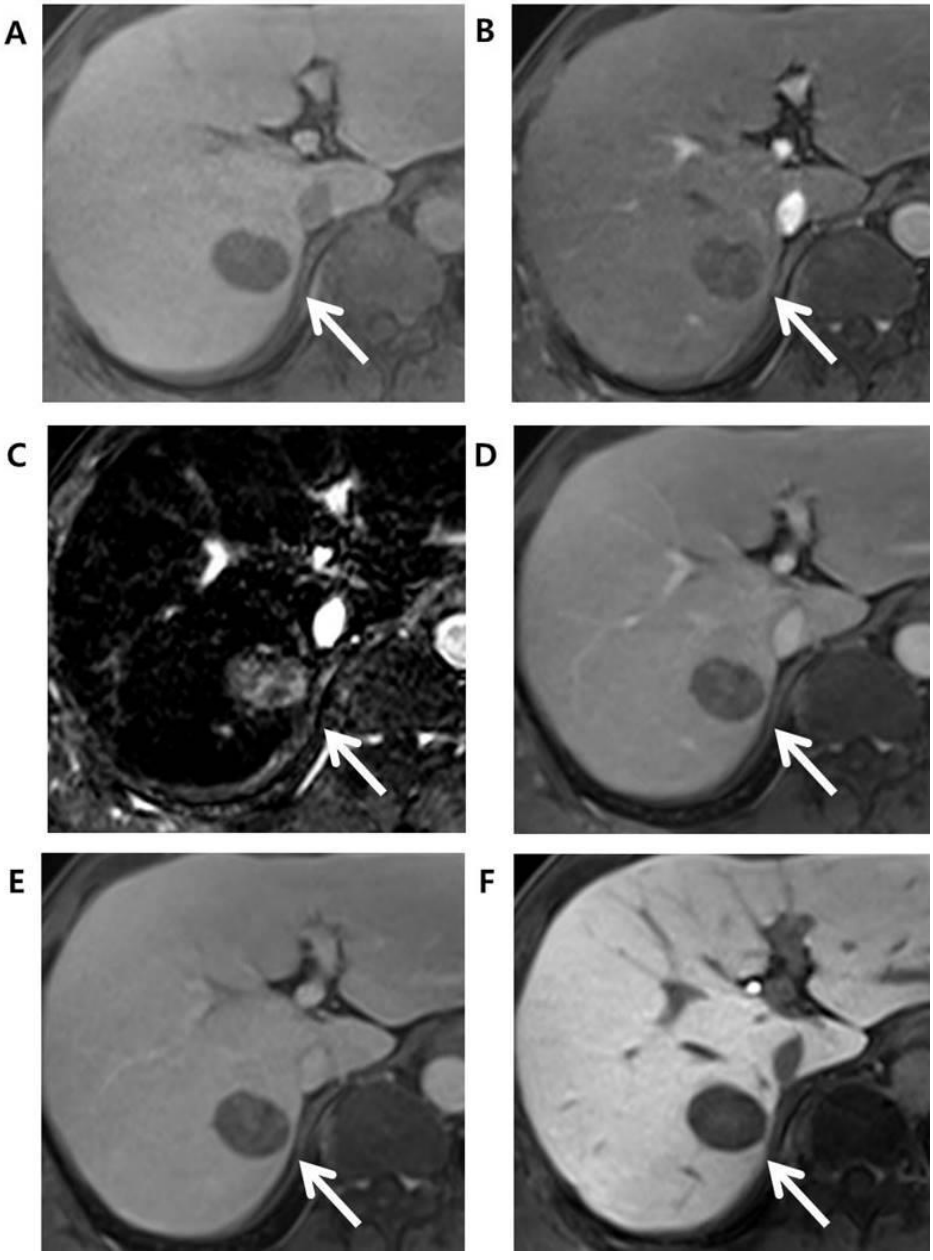

Figure 2. Edmonson grade 3 HCC in 49-year-old male with underlying chronic B-viral infection. Compared to the (A) axial pre-contrast phase, the (B) late arterial phase (AP), and (D) portal venous phase (PVP) images after gadoxetate administration showed a 30mm-sized liver mass (arrow) in segment 7 (S7) of the liver with no nonrim arterial

hyperenhancement in the late arterial phase but washout in the portal venous phase. Initially, this hepatic observation was categorized as LR-4. (C) The arterial subtraction image, however, showed homogeneous enhancement compared to the normal liver parenchyma. This hepatic observation was thus recategorized as LR-5 based on the arterial subtraction image. (E) Delayed phase and (F) hepatobiliary (HBP) phase images showed decreased signal intensity in the hepatic observation compared to liver parenchyma.

Similarly, among 73 LR-M observations, one observation showed iso-to-hypointensity with peripheral rim enhancement in late arterial phase but a homogenous hyperenhancement in the subtraction image. The final LR category of this observation was adjusted to LR-5 from LR-M and was also confirmed as HCC. The adjusted LR-5 showed a sensitivity of 74.4% and a specificity of 97.9% for HCC, and a significant difference was noted in sensitivity (P<0.001) but not in specificity (P>0.999) when compared to original LR-5 (Table 2).

E. Diagnostic performance of LR-5 for HCC considering no washout if APHE was absent

Out of 81 HCCs that showed no APHE, 77 (95.1%) HCCs showed washout in portal venous phase. When washout was considered absent because APHE was absent, three LR-5 observations were readjusted to LR-4. Diagnostic performance of LR-5 after this adjustment showed a sensitivity of 71.3% (P=0.250) and a specificity of 97.9% (P>0.999).

F. Diagnostic performance of LR-5 for HCC after extending washout to the transitional phase image (transitional phase hypointensity as a major feature)

Out of 76 HCCs that did not show washout in portal venous phase, 39 (51.3%) showed hypointensity in the transitional phase. Based on LI-RADS v2018, 20 observations were assigned LR-4, 16 observations were assigned LR-5 and three

observations were assigned LR-M. When transitional phase hypointensity was also considered to indicate washout, a major feature, 19 LR-4 observations were readjusted to LR-5, resulting in 1 LR-4 and 35 LR-5. Diagnostic performance of adjusted LR-5 showed a sensitivity of 75.6% (P<0.001) and a specificity of 96.8% (P=0.250) (Table 2).

G. Diagnostic performance of LR-5 for HCC when subthreshold growth was considered a major feature similar to threshold growth in LI-RADS v2017

Among the total 551 LR-3, -4, and -5 observations, 34 observations (6.2%) showed subthreshold growth wherein 30 of these 34 observations (88.2%) were histopathologically confirmed as HCC. Initially, the final LR-categories of the 34 observations were LR-4 for 26 observations and LR-5 for 8 observations. However, when subthreshold growth was regarded as a major feature as it was in LI-RADS v2017, 15 LR-4 observations were readjusted to LR-5. This category-adjusted LR-5 showed a sensitivity of 74.8% and a specificity of 97.9% (Table 2). Compared to original LR-5, significant increase in sensitivity (P<0.001) and non-significant decrease in specificity (P>0.999) were noted.

2. Threshold growth as a major feature in the diagnosis of HCC

A. Patient characteristics and pathologic findings

Out of 1,017 patients who were identified based on the inclusion and exclusion criteria, 4 patients with tumor-in-vein were removed which resulted in a total of 1,013 patients in the final analysis (Figure 3). Clinico-pathologic characteristics of these 1,013 patients (775 men and 238 women; median age, 56 years) are summarized in Table 4. Out of 1,013 patients, 677 patients underwent following surgeries: 99 patients underwent wedge resection, 256 and 291 patients received segmentectomy and lobectomy, respectively, and 31 patients underwent liver transplantation.

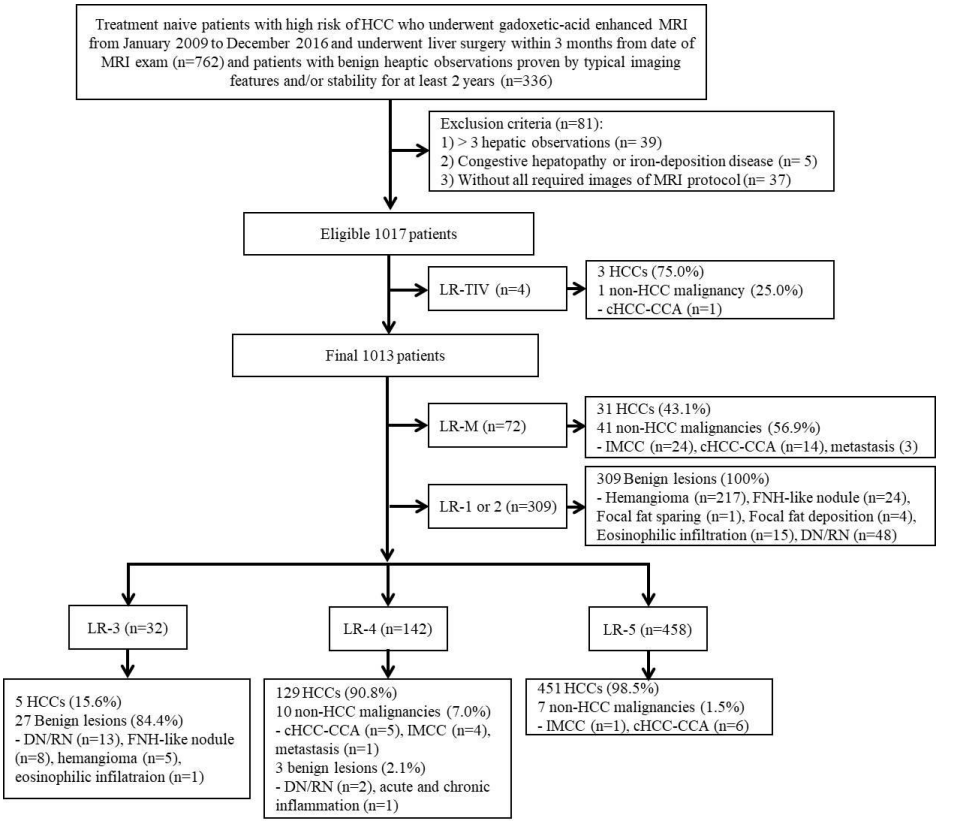

Figure 3. Inclusion and exclusion criteria of study population and original final LR-categories of the study population based on LI-RADS v2018.

Table 4. Clinical-pathologic characteristics of patients and hepatic observations

Characteristics	Value
Patients (n= 1,013)	
Median age (y)*	56 (13)
Sex	
Men	775 (76.5)
Women	238 (23.5)
Cause of liver disease	
Hepatitis B virus	875 (86.4)
Alcohol	78 (7.7)
Hepatitis C virus	34 (3.4)
NASH	8 (0.8)
Autoimmune	1 (0.1)
Unknown	17 (1.7)
Number of observations per patient	

1	825 (81.4)
2	99 (9.8)
3	89 (8.8)
Lesions (n=1,013)	
Median size (mm)**	24.1 (21.9)
HCC	29.3 (21.1)
Non-HCC malignancies	36.2 (22.6)
Benign lesions	11.0 (8.0)
Size subgroup	
<10mm	82 (8.1)
10-19mm	315 (31.1)
≥20mm	616 (60.8)
Final diagnosis	
HCC	616 (60.8)
Non-HCC malignancies	58 (5.7)
iCCA	29 (50.0)
cHCC-CCA	24 (41.4)
Metastasis	4 (6.9)
Sarcomatoid cHCC-CCA	1 (1.7)
Benign tumors	339 (33.5)
Hemangioma	222 (65.5)
Dysplastic or regenerative nodule	63 (18.6)
FNH-like nodule	32 (9.4)
Eosinophilic infiltration	16 (4.7)
Focal fat deposition	4 (1.2)
Focal fat sparing	1 (0.3)
Inflammatory pseudotumor	1 (0.3)
Pathologically confirmed liver fibrosis (n=677)	
Cirrhosis (Grade 4)	405 (59.8)
Septal fibrosis (Grade 3)	134 (19.8)
Periportal fibrosis (Grade 2)	102 (15.1)
Portal fibrosis (Grade 1)	36 (5.3)
Median time interval between MRI and pathologic diagnosis (d)**	13 (15)

Note- Unless stated otherwise, data are number of patients or observations. Data in parentheses are percentages.
Abbreviations: cHCC-CCA, combined HCC-choangiocarcinoma; FNH, focal nodular hyperplasia; HCC, hepatocellularcarcinoma; iCCA, intrahepatic mass-forming cholangiocarcinoma; NASH, non-alcoholic steatohepatitis; y, years; d, days
*Data are presented as median values. Data in parentheses are interquartile ranges and were calculated as the difference between the 75th and 25th percentiles.

The total 1,013 hepatic observations consisted of 616 HCCs, 58 non-HCC malignancies (29 iCCA, 24 cHCC-CCA, 4 metastasis from ovarian epithelial cancer, pancreatic adenocarcinoma and colon adenocarcinoma, and 1 sarcomatoid

cHCC-CCA) and 339 benign tumors (222 hemangioma, 63 dysplastic or regenerative nodules, 32 FNH-like nodules, 16 eosinophilic infiltrations, 4 focal fat deposition, 1 focal fat sparing and 1 acute and chronic inflammatory lesion). Median sizes of HCC and non-HCC malignancies were 29.3mm and 36.2mm, respectively. In addition, out of 405 patients with liver cirrhosis, 230 patients had Child Pugh class A, 173 patients had Child-Pugh class B, and 2 patients had Child-Pugh class C.

B. Frequency of threshold growth and correlation to size of hepatic observation

Out of the total 674 patients with hepatic malignancies, 23 (39.7%) out of 58 patients with non-HCC malignancies and 119 (19.3%) out of 616 patients with HCCs had prior exam taken within 6 months from the date of the MRI. Out of these 142 patients with prior exams, 15 had prior exam within 1 month of date of MRI, 92 had prior exam 1-3 months before date of MRI, and 35 had prior exams 3-6 months before date of MRI. All of the patients with prior exams 1 to 6 months prior to date of MRI underwent MRI as follow-up to check interval size change while most of the patients with prior exam taken within 1 month from date of MRI underwent MRI for further characterization. Among patients with prior exams, however, threshold growth was more frequent in non-HCC malignancies compared to HCCs (P<0.001) (Table 5).

Table 5. Correlation between observation size and theshold growth

	# of patients with ≤6months CT/MR	Threshold growth (+)	Threshold growth (-)	P-value[a]	P-value[b]
HCC (n=616)					
<10mm	3/8 (37.5%)	0/3 (0.0%)	3/3 (100.0%)	0.360	0.607
10-19mm	27/114 (23.7%)	6/27 (22.2%)	21/27 (77.8%)		
≥20mm	89/494 (18.0%)	11/89 (12.4%)	78/89 (87.6%)		
Non-HCC malignancies (n=58)					
<10mm	3/3 (100.0%)	3/3 (100.0%)	0/3 (0.0%)	0.199	0.090
10-19mm	4/6 (66.7%)	2/4 (50.0%)	2/4 (50.0%)		
≥20mm	16/49 (32.7%)	6/16 (37.5%)	10/16 (62.5%)		

Abbreviations: HCC, hepatocellular carcinoma
P-value[a]: Fisher's exact test
P-value[b] : Cochran-Armitage's trend test

The mean size of non-HCC malignancies with threshold growth (22.2±14.2mm; range: 9.0-48.6mm) was significantly smaller than the mean size of non-HCC malignancies without threshold growth (42.9 ± 28.2mm; range: 12.4-120.4mm) (*P*=0.040). There was no significant correlation between size range of non-HCC malignancies (i.e. <10mm, 10-19mm, and ≥20mm) and threshold growth (*P*=0.090). As for HCC, the mean size of HCC with threshold growth (26.8±12.9mm; range: 11.7-60.7mm) was also smaller than the mean size of HCC without threshold growth (33.1±18.6mm; range: 7.0-140.0mm) but this difference was not statistical significant (*P*=0.184). Furthermore, smaller HCC did not show tendency for more threshold growth as there was no significant correlation between HCC size and threshold growth (*P*=0.607) (Table 5, Figure 4).

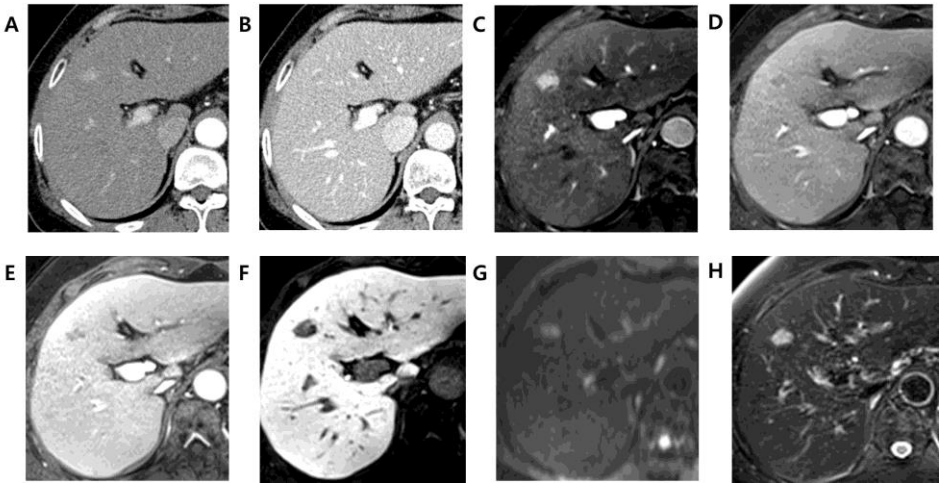

Figure 4. 61 year-old woman with Edmonson grade II HCC. Liver dynamic CT (A-B) taken on January 2nd, 2009 with (A) non-rim arterial phase hyperenhancement (APHE) in arterial phase and (B) washout in portal venous phase. Gadoxetate-enhanced liver dynamic MRI (C-H) taken on February 27th, 2009 (about 2 months later from prior

exam) with (C) APHE in late arterial phase, (D) washout with capsular enhancement in portal venous phase, (E) transitional phase hypointensity, (F) hepatobiliary phase hypointensity, (G) diffusion restriction in diffusion-weighted imaging (DWI) and (H) moderate T2 hyperintensity in T2-weighted image. This observation′s longest diameter measured 12mm in liver dynamic CT and measured 15mm in gadoxetate enhanced MRI and thus no presence of threshold growth was noted.

C. Changes to final LR-category before and after follow-up exam.

Out of 144 patients with prior exams, the final LR-category changed in 11 (7.6%) patients (Table 6). Four patients (patients #1-#4) showed threshold growth in MRI and had their LR-categories changed due to added major criterion. In case of patient #3, presence of threshold growth allowed the final LR-category to upgrade to LR-5 in follow-up MRI even though the pathology was later confirmed as combined hepatocellular cholangiocarcinom, a non-HCC malignancy (Figure 5). LR-categories of six patients (patients #5-10) were upgraded as the tumor size increased to ≥20mm in MRI. One patient (patient #11) had LR-category upgraded from LR-3 to LR-4 in MRI due to ancillary features such as transitional phase hypointensity and hepatobiliary phase hypointensity, which could not be assessed in prior CT exam.

Table 6. Patients with prior exams within 6 months of the date of MRI whose final LR-category changed before and after follow-up exams with MRI findings, lesion size and corresponding LR-category change

	Size (mm) (CT)	Size (mm) (MR)	APHE	WO	CE	TG	LR change
Patient #1	7	13	X	O	X	O	LR3 -> LR4
Patient #2	14	24	O	X	X	O	LR3 -> LR5
Patient #3	9	23	O	X	X	O	LR3 -> LR5
Patient #4	13	24	O	X	X	O	LR3 -> LR5
Patient #5	17	21	X	O	X	X	LR3 -> LR4

Patient #6	18	25	X	O	X	X	LR3 -> LR4
Patient #7	17	21	O	X	X	X	LR3 -> LR4
Patient #8	19	24	O	X	X	X	LR3 -> LR4
Patient #9	18	23	O	X	O	X	LR4 -> LR5
Patient #10	17	22	O	X	X	X	LR3 -> LR4
Patient #11	8	11	O	X	X	X	LR3 -> LR4

Abbreviations: APHE, (nonrim) arterial phase enhancement; CE, capsular enhancement; TG, threshold growth; WO, washout; LR, LI-RADS.
All of the above patients' prior exam before MRI were liver dynamic CT exams.
O = presence of corresponding major feature
X = absence of corresponding major feature

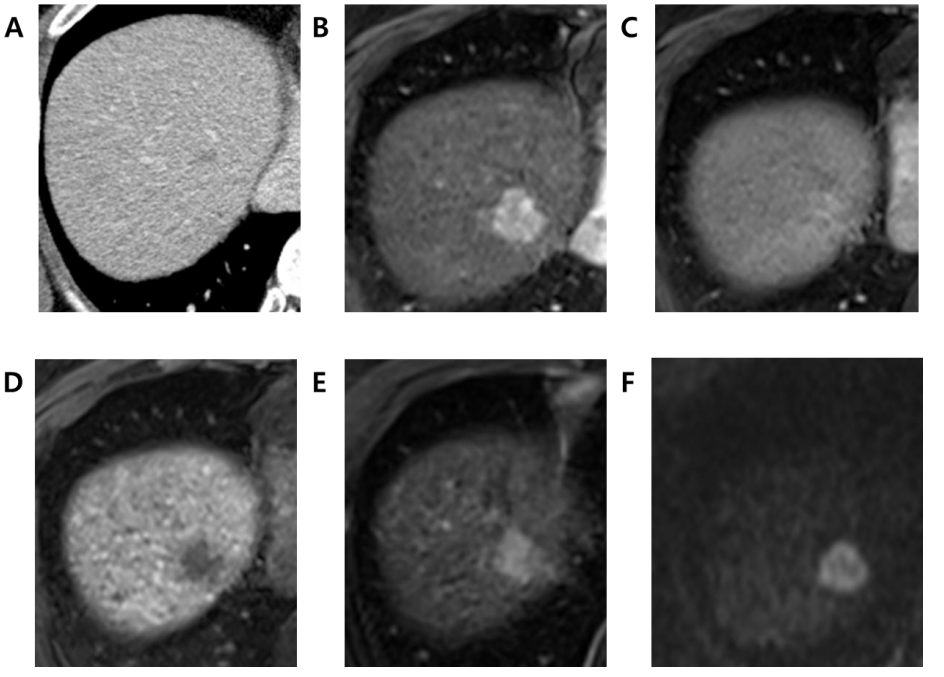

Figure 5. 34 year-old man with combined hepatocellular-cholangiocarcinoma. (A) Portal venous phase of abdominal CT taken on December 27th, 2008 shows focal hypodense lesion measuring less than 1cm in longest diameter. Gadoxetate enhanced MRI taken on June 7th, 2009 (about six months later from prior exam) with (B) late

arterial phase, (C) portal venous phase, (D) hepatobiliary phase, (E) T2- weighted image and (F) diffusion-weighted imaging (DWI). This observation shows non-rim enhancement in arterial phase without definite washout, hepatobiliary phase hypointensity, moderate T2 hyperintensity and diffusion restriction. This observation measured 2.3cm in longest diameter in gadoxetate enhanced MRI, thus showing presence of threshold growth and was assigned LR-5 in MRI.

D. Frequency of major and ancillary features in HCC and non-HCCs.

As expected, APHE, washout, and enhancing capsule were more frequently observed in HCCs compared to non-HCC malignancies with significant difference (*Ps*<0.001) (Table 7).

Table 7. Frequency of major and ancillary features in non-HCC malignancies and HCC.

	Data available	**non-HCC malignancies (n=58)**	**HCC (n=616)**	***P*-value***
Major features				
APHE (arterial phase hyperenhancement)	674	18 (31.0 %)	521 (84.5%)	<0.001
WO (washout)	674	19 (32.7%)	489 (79.3%)	<0.001
Enhancing capsule	674	5 (8.6%)	181 (29.4%)	<0.001
Threshold growth	142	11/23 (47.8%)	17/119 (14.2%)	<0.001
Ancillary features				
Subthreshold growth	53	5/7 (71.4%)	36/46 (78.3%)	0.704
Targetoid mass features	674	32 (55.2%)	27 (4.4%)	<0.001
Corona enhancement	674	22 (37.9%)	134 (21.8%)	0.005
Fat sparing in solid mass	674	1 (1.7%)	13 (2.1%)	0.844
Restricted diffusion	674	55 (94.8%)	585 (95.0%)	0.963
Mild to moderate T2 hyperintensity	674	53 (91.4%)	579 (94.0%)	0.431
Iron sparing in solid	674	0 (0%)	3 (0.5%)	>0.999

mass				
TP (transitional phase) hypointensity	674	47 (81.0%)	562 (91.2%)	0.012
HBP (hepatobiliary phase) Hypointensity	674	54 (93.1%)	574 (93.2%)	0.982
Nonenhancing capsule	674	2 (3.4%)	27 (4.4%)	>0.999
Nodule-in-nodule	674	0 (0%)	7 (1.1%)	>0.999
Mosaic architecture	674	2 (3.4%)	50 (8.1%)	0.203
Fat-in-nodule	674	2 (3.4%)	99 (16.1%)	0.010
Blood product	674	2 (3.4%)	56 (9.1%)	0.217

*Chi-square test or Fisher's exact test.
Abbreviations: HCC, hepatocellular carcinoma

For the ancillary features, targetoid mass features and corona enhancement were significantly more frequent in non-HCC malignancies. Within ancillary features favoring HCC in particular, transitional phase hypointensity and fat-in-nodule were more significantly frequent in HCCs.

E. Diagnostic performance of adjusted LR-5 after modifying major features using ancillary features

The final LR categories of the total 1,013 patients based on LI-RADS v2018 were as follows: 72 LR-M, 309 LR-2, 32 LR-3, 144 LR-4 and 458 LR-5 (Figure 3). Based on these categorizations, LR-5 showed sensitivity of 73.2% and specificity of 98.2% for HCC (Table 8).

Table 8. Sensitivity, specificity, accuracy, positive predictive value (PPV) and negative predictive value (NPV) of HCC under various adjustment of major and ancillary features in LI-RADS v2018

	Sensitivity (%)	**Specificity (%)**	**PPV (%)**	**NPV (%)**	**Accuracy (%)**	***P*-value[a]**	***P*-value[b]**
LIRADS v2018							
LR-5	73.2 (451/616) [69.5, 76.7]	98.2 (390/397) [96.4, 99.3]	98.5 (451/458) [96.9, 99.3]	70.3 (390/555 [67.5, 72.9]	83.0 (841/1013) [80.6, 85.3]	-	-
Fat- in-nodule as an additional major feature							

LR-5	73.9 (455/616) [70.2, 77.3]	98.2 (390/397) [96.4, 99.3]	98.5 (455/462) [96.9, 99.3]	70.8 (390/551) [68.0, 73.5]	83.4 (845/1013) [81.0, 85.7]	0.125	>0.999
Fat-in-nodule replaces threshold growth as major feature*							
LR-5	73.9 (455/616) [70.2, 77.3]	98.5 (391/397) [96.7, 99.4]	98.7 (455/461) [97.2, 99.4]	70.8 (391/552) [68.0, 73.5]	83.5 (846/1013) [81.1, 85.8]	0.289	>0.999

Abbreviations: HCC, hepatocellular carcinoma; LI-RADs, Liver Imaging Reporting and Data SystemsDiagnostic performance of LR-5 if fat-in-nodule is added as a major feature or replaces threshold growth are compared to the original diagnostic performance of LR-5 based on LI-RADS v2018.
Numbers in parentheses are the 95% confidence intervals (CIs).
[a]*P*-value after comparing sensitivity to sensitivity of original LR-5 using McNemar's test
[b]*P*-value after comparing specificity to specificity of original LR-5 using McNemar's test
*Threshold growth was considered as an ancillary feature.

Although the presence of transitional phase hypointensity was significantly different between non-HCC malignancies and HCCs (*P*=0.012), the presence of this finding was high in both non-HCC malignancies (47/58, 81.0%) and HCC (562/616, 91.2%) and could not be considered as a useful imaging feature for the differential diagnosis of HCC. Since fat-in-nodule was more significantly frequent in HCCs compared to non-HCC malignancies (*P*=0.010) and was only seen 3.4% of non-HCC malignancies, it was selected as a possible candidate as additional or replacing major feature.

After adding fat-in-nodule to major features, 4 LR-4 observations were upgraded to LR-5 and the LR-5 sensitivity increased without statistical significance to 73.9% (*P*=0.125) while no change was noted for LR-5 specificity for HCC (Table 8).

When fat-in-nodule replaced threshold growth as a major feature and threshold growth was considered as an ancillary feature, 7 LR-4 observations were upgraded to LR-5 while 3 LR-5 observations were downgraded to LR-4. Under this condition, LR-5 sensitivity and specificity were 73.9% (*P*=0.289) and 98.5% (*P*>0.999).

F. Correlation between observation size and Edmondson grade of HCC and

threshold growth

No significant correlation was found between threshold growth and Edmondson grade of HCC (*P*=0.364) and no trend was found between threshold growth in either lower or higher Edmondson grade HCC (*P*=0.637) (Table 9).

Table 9. Correlation between Edmondson grade of HCC and threshold growth

	Edmonson grade				*P*-value[1]	*P*-value[2]
	1	2	3	4		
Threshold growth	3 (17.7%)	10 (58.8%)	4 (23.5%)	0 (0%)	0.364	0.637

P-value[1]: Fisher's exact test
P-value[2]: Cochran-Armitage's trend test
Abbreviation: HCC, hepatocellular carcinoma

3. Usefulness of hepatobiliary phase signal intensity in the diagnosis of HCC with atypical imaging features among LR-M observations

A. Diagnostic performance of combined LR-4 and LR-5, LR-5 and LR-M

Based on the eligibility criteria, final LR-categories were assigned to 1288 observations based on LI-RADS v2018 [7] and are summarized in Figure 6. Overall the sensitivity and specificity of LR-4 and LR-5 combined, and LR-5 were 92.9% and 94.9%, and 71.6% and 98.3%, respectively (Table 10).

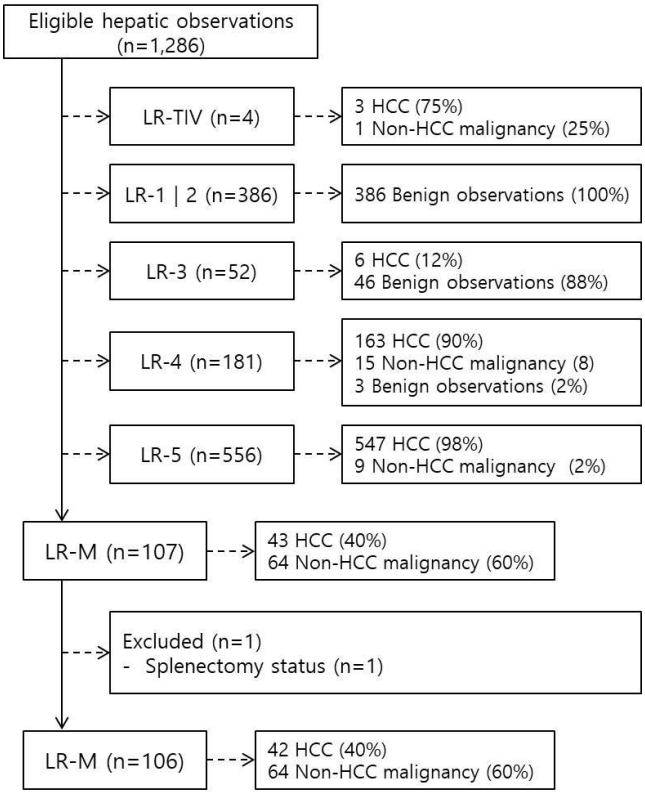

Figure 6. Flow diagram of hepatobiliary phase signal intensity study. HCC, hepatocellular carcinoma

Table 10. Sensitivity, specificity, positive predictive value (PPV), negative predictive value and accuracy for HCC based on LI-RADS v2018 of eligible hepatic observations

	Sensitivity (%)	**Specificity (%)**	**PPV (%)**	**NPV (%)**	**Accuracy (%)**	***P*-value**
LR-4 and LR-5 combined	92.9 (710/764) [90.9, 94.7]	94.9 (497/524) [92.6, 96.6]	96.3 (710/737) [94.8, 97.4]	90.2 (497/551) [87.7, 92.3]	93.7 (1207/1288) [92.2, 95.0]	<0.001
LR-5	71.6 (547/764) [68.3, 74.8]	98.3 (515/524) [97.8, 99.2]	98.4 (547/556) [97.0, 99.2]	70.4 (515/732) [67.9, 72.7]	82.5 (1062/1288) [80.3, 84.5]	<0.001

*Sensitivity, specificity, PPV, NPV and accuracy for LR-M is calculated for non-HCC malignancy not HCC.
HCC, hepatocellular carcinoma; LI-RADS, Liver Imaging-Reporting and Data System; PPV, positive predictive value; NPV, negative predictive value

B. Baseline clinical characterisitics of LR-M patients

Baseline patient characteristics are summarized in Table 11 and Table 12. Our 106 LR-M patients comprised of 78 males and 28 females with mean age of 60 ± 11.5 years old. Chronic hepatitis B was the most predominant cause of underlying liver disease (80% of patients) and 48% had cirrhosis. Most patients (97%) were of Child Pugh class A and mean size of tumor was 38mm. The median duration between MRI and surgical pathology was 17 days.

Table 11. Baseline characteristics of the included patients

Variables	**Total patients (*n= 106*, 100%)**	**HCC (*n=42*, 40%)**	**Non-HCC malignancy (*n= 64*, 60%)**	***P*-value**
Age, years	60.0 ± 11.5	56.2 ± 12.0	62.6 ± 10.6	**0.005**
Sex				0.290
Male	78 (74)	34 (81)	44 (69)	
Female	28 (26)	8 (19)	20 (31)	
Etiology				
Hepatitis B	85 (80)	38 (91)	47 (73)	**0.025**
Hepatitis C	3 (3)	0 (0)	3 (5)	0.270
Alcohol	12 (11)	2 (5)	10 (16)	0.117
NASH	6 (6)	2 (5)	4 (6)	0.999
Child-Pugh Class				0.999
A	103 (97)	41 (98)	62 (97)	
B	3 (3)	1 (2)	2 (3)	
Cirrhosis	51 (48)	25 (60)	26 (41)	0.088
AST, IU/L	27 (21 – 40)	27 (21 – 44)	27 (21 – 38)	0.543
ALT, IU/L	25 (18 – 40)	31 (24 – 44)	22 (15 – 38)	**0.002**
Albumin, g/dL	4.3 (4.1 – 4.6)	4.5 (4.1 – 4.6)	4.2 (3.9 – 4.5)	**0.034**
Total bilirubin (mg/dL)	0.7 (0.5 – 1.0)	0.8 (0.6 – 1.1)	0.7 (0.5 – 0.9)	
PT, INR	0.98 (0.94 – 1.03)	0.98 (0.94 – 1.01)	0.98 (0.93 – 1.05)	0.837
Platelets, 1000/μL	208.4 ± 88.8	184.5 ± 61.0	224.8 ± 100.8	**0.012**
AFP, IU/mL	5.1 (2.7 – 51.9)	6.2 (3.5 – 156.2)	3.5 (2.5 – 14.9)	**0.019**
PIVKA-II, AU/mL	31.0 (20.0 – 121.0)	47.0 (24.0 – 282.0)	26.0 (18.0 – 37.0)	**0.003**
CA 19-9, U/mL	24.8 (8.4 –	6.9 (0.1 – 13.4)	37.8 (15.3 –	**<0.001**

	123.0)		392.0)	
CEA, ng/mL	2.9 (1.7 – 4.8)	2.9 (1.6 – 3.9)	2.9 (1.8 – 6.0)	0.272
Observation size, mm	38.6 ± 20.4	34.4 ± 16.1	41.4 ± 22.5	0.083
Duration between MRI and surgical pathology, days	17 (10 – 28)	16 (8 – 24)	18 (11 – 33)	0.190
BCLC stage 0		8 (19)		
BCLC stage A		34 (81)		

Numerical variables are expressed as median (interquartile range) or mean ± standard deviation, according to the result of normality test (Shapiro-Wilk test). Categorical variables are expressed as *n* (%). BCLC, Barcelona Clinic Liver Cancer; HCC, hepatocellular carcinoma; NASH, non-alcoholic steatohepatitis; AST, aspartate transaminase; ALT, alanine transaminase; AFP, α-fetorprotein; PIVKA, protein induced by vitamin K absence; CA 19-9, carbohydrate antigen 19-9; CEA, carcinoembryonic antigen; MRI, magnetic resonance imaging.

Table 12. Comparison of baseline characteristics of HCC, cHCC-CCA and CCA

Variables	**HCC (*n=42*, 40%)**	**cHCC-CCA (*n=22*, 21%)**	**iCCA (*n=39*, 37%)**	***P*-value**	***P*-value[a]**	***P*-value[b]**	***P*-value[c]**
Age, years	56.2 ± 12.0	59.5 ± 9.6	64.8 ± 10.9	**0.005**	0.214	0.059	**0.002**
Sex				0.520			
Male	34 (81)	17 (77)	26 (67)				
Female	8 (19)	5 (23)	13 (33)				
Etiology							
Hepatitis B	38 (91)	17 (77)	28 (72)	0.075			
Hepatitis C	0 (0)	0 (0)	3 (8)	0.071			
Alcohol	2 (5)	3 (14)	6 (15)	0.237			
NASH	2 (5)	2 (9)	2 (5)	0.757			
Child-Pugh Class				0.874			
A	41 (98)	21 (96)	37 (97)				
B	1 (2)	1 (5)	1 (3)				
Cirrhosis	25 (60)	13 (59)	12 (31)	**0.019**	0.941	0.057	**0.014**
AST, IU/L	27 (21 – 44)	29 (23 – 58)	27 (20 – 35)	0.180			
ALT, IU/L	31 (24	27 (20	21 (13	**0.002**	0.325	**0.036**	**<0.001**

	– 44)	– 42)	– 34)				
Albumin, g/dL	4.5 (4.1 – 4.6)	4.2 (3.9 – 4.6)	4.3 (4.0 – 4.4)	0.133			
Total bilirubin, mg/dL	0.8 (0.6 – 1.1)	0.8 (0.7 – 1.0)	0.7 (0.4 – 0.9)	0.070			
PT, INR	0.98 (0.94 – 1.01)	1.01 (0.93 – 1.07)	0.97 (0.92 – 1.03)	0.683			
Platelets, 1000/μL	184.5 ± 61.0	155.0 ± 65.0	223 ± 107.6	**<0.001**	0.230	**<0.001**	**<0.001**
AFP, IU/mL	6.2 (3.5 – 156.2)	11.6 (2.7 – 106.4)	2.9 (2.2 – 4.5)	**0.001**	0.967	**0.002**	**<0.001**
PIVKA-II, AU/mL	47.0 (24.0 – 282.0)	28.5 (16.0 – 69.8)	25.0 (18.0 – 34.0)	**0.008**	0.048	0.402	0.004
CA 19-9, U/mL	6.9 (0.1 – 13.4)	10.6 (8.7 – 36.7)	95.0 (23.7 – 1478.0)	**<0.001**	**0.014**	**0.016**	**<0.001**
CEA, ng/mL	2.9 (1.6 – 3.9)	3.2 (1.8 – 4.9)	2.7 (1.8 – 5.8)	0.544			
Observation size, mm	34.4 ± 16.1	39.1 ± 16.5	36.8 ± 26.0	0.316			
Duration between MRI and surgical pathology, days	16 (8 – 24)	19 (10 –24)	21 (12 – 37)	0.119			

Numerical variables are expressed as median (interquartile range) or mean ± standard deviation, according to the result of normality test (Shapiro-Wilk test). Categorical variables are expressed as *n* (%). HCC, hepatocellular carcinoma; iCCA, intrahepatic mass-forming cholangiocarcinoma; cHCC-CCA, combined hepatocellular-cholangiocarcinoma; NASH, non-alcoholic steatohepatitis; AST, aspartate transaminase; ALT, alanine transaminase; AFP, α-fetorprotein; PIVKA, protein induced by vitamin K absence; CA 19-9, carbohydrate antigen 19-9; CEA, carcinoembryonic antigen; MRI, magnetic resonance imaging.

[a]Pair-wise comparison between HCC and cHCC-CCA

[b]Pair-wise comparison between cHCC-CCA and iCCA

[c]Pair-wise comparison between HCC and iCCA

Within 106 LR-M patients, 42 patients (40%) were HCCs and 64 patients (60%) were non-HCC malignancies. Most HCC patients (34/42, 81%) were of Barcelona Clinic Liver Cancer (BCLC) stage A and the rest were of BCLC stage 0.

Patients with non-HCC malignancies showed significantly older age (mean age: 62.6 vs. 56.2, *P*=0.005), fewer underlying chronic hepatitis B background (73% vs. 91%, *P*=0.025), lower alanine transaminase (ALT) (22.0 vs. 32.0, *P*=0.002), α-fetoprotein (3.5 vs. 6.2, *P*=0.019), PIVKA-II (26.0 vs. 47.0, *P*=0.003) and higher CA19-9 (37.8 vs. 6.9, *P*<0.001) compared to patients with HCC (Table 11).

Subgroup analysis of non-HCC malignancies showed that 21% (22/64) had cHCC-CCA while 37% (39/64) had iCCA (Table 12). The remaining three patients had metastases: one ovarian cancer metastasis and two colon cancer metastases.

Subgroup analysis of LR-M observations showed that the significant differences in age, albumin, α-fetoprotein, and CA19-9 between HCC with atypical imaging features and non-HCC malignancies were mainly due to significant differences between HCC and iCCA: age (*P*=0.002), underlying cirrhosis (*P*=0.014), albumin (*P*<0.001), α-fetoprotein (*P*<0.001) and CA19-9 (*P*<0.001) (Table 12). While CA19-9 was significantly different across HCC, cHCC-CCA and iCCA (*P*<0.001), all other factors were not found statistically significant in differentiating HCC from cHCC-CCA.

C. Hepatobiliary phase signal intensity classification of HCC and non-HCC malignancies.

Out of 106 LR-M observations, 42 observations (42%) were assigned dark, 61 observations (58%) were assigned low, and 3 observations (3%) were assigned iso-to-high signal intensities in hepatobiliary phase. Figure 7 and Figure 8 shows typical images of LR-M observation with dark, low and iso-to-high signal intensity in hepatobiliary phase. Nearly half of 42 dark observations (22, 51%) were found to be HCC while 23% (10/42) and 19% (8/42) were found to be iCCA and cHCC-CCA, respectively (Table 13). Significant associations between HCC and dark signal intensity over low signal intensity (*P*=0.036) as well as between iCCA or cHCC-CCA or iCCA

and low signal intensity over dark signal intensity (*P*s<0.05) were found (Table 13). These associations were found significant under univariate analyses as well (Table 14 and Table 15). In case of iso-to-high observations, all three observations were found to be HCC although this association was not found to be statistically significant (*P*=0.060) (Table 16). Not a single cHCC-CCA, iCCA or metastasis was found to be iso-to-high in hepatobiliary phase.

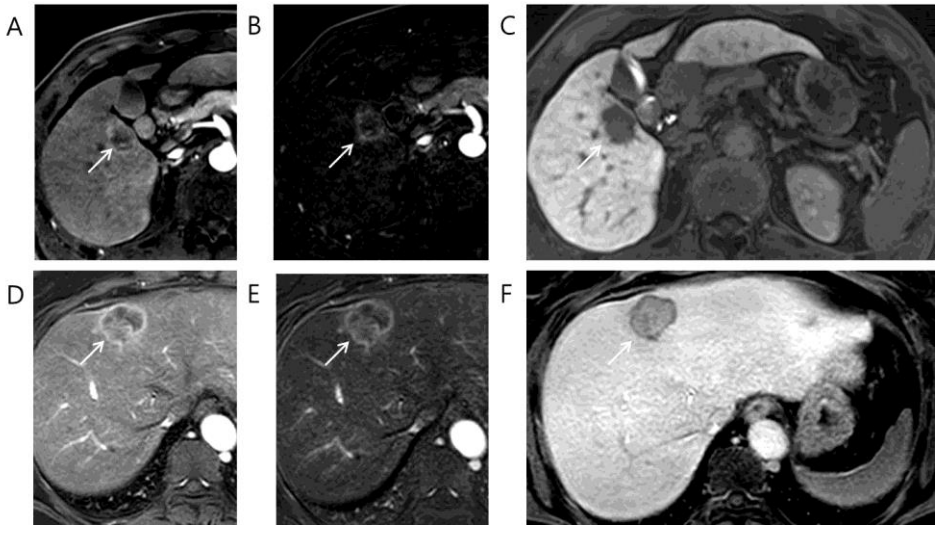

Figure 7. 46 year old male patient with Edmondson grade III HCC (A-C): rim APHE in (A) late arterial phase and (B) arterial subtraction image, (C) dark signal intensity in hepatobiliary phase. 58 year old female patient with moderately differentiated cHCC-CCA (D-F): rim APHE in (D) late arterial phase, and (E) arterial subtraction image, (F) low signal intensity in hepatobiliary phase.

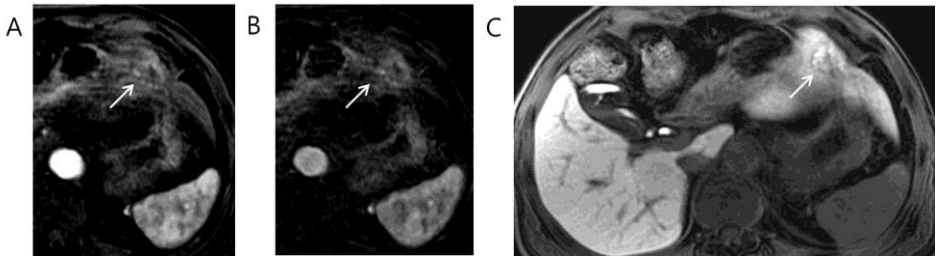

Figure 8. 73 year old male patient with Edmondson grade I HCC. Rim APHE is shown in (A) late arterial phase, (B) arterial subtraction image and (C) hepatobiliary phase. This hepatic observations shows iso-to-high signal intensity in hepatobiliary phase.

Table 13. Hepatobiliary phase (HBP) signal intensities of HCC and non-HCC malignancies.

HBP Signal intensity	Dark	Low	Iso-to-High	***P*-value***	***P*-value[a]**	***P*-value[b]**	***P*-value[c]**
HCC (*n=42*, 40%)	22 (52)	17 (41)	3 (7)	**0.004**	**0.036**	0.081	0.242
cHCC-CCA (*n=22*, 21%)	8 (36)	14 (64)	0 (0)	0.595	0.635	0.999	0.999
iCCA (*n=39*, 37%)	10 (26)	29 (74)	0 (0)	**0.026**	**0.045**	0.245	0.999
cHCC-CCA or iCCA *(n=61*, 58%)	18 (29)	43 (71)	0 (0)	**0.001**	**0.015**	0.096	0.264
Metastasis (n=*3*, 3%)	2 (67)	1 (33)	0 (0)	0.615	0.565	0.999	0.999

Categorical variables are expressed as *n* (%). HBP, hepatobiliary phase; HCC, hepatocellular carcinoma; iCCA, intrahepatic mass-forming cholangiocarcinoma; cHCC-CCA, combined hepatocellular-cholangiocarcinoma
Dark: signal intensity lower than spleen parenchyme
Low: signal intensity higher than spleen parenchyme but lower than liver parenchyme
Iso: signal intensity similar to liver parenchyme
High: signal intensity higher than liver parenchyme
**P*-value calculated via X^2- test or Fisher's exact test comparing three groups (signal intensity) for each malignancy
[a]Pairwise comparison between dark group and low group
[b]Pairwise comparison between low group and iso-to-high group
[c]Pairwise comparison between dark group and iso-to-high group

Table 14. X^2-test result HCC vs. dark signal intensity group in hepatobiliary phase

	Low, and iso-to-high SI	Dark SI	*P*-value
Non-HCC LR-M (n=64)	44	20	**0.030**
HCC LR-M (n=42)	20	22	

HCC, hepatocellular carcinoma; SI, signal intensity.

Table 15. X^2-test result iCCA or cHCC-CCA vs. low signal intensity group in hepatobiliary phase

	Dark, and iso-to-high SI	Low SI	*P*-value
Rest of LR-M (n=45)	27	18	**0.002**
iCCA or cHCC-CCA (n=61)	18	43	

iCCA, intrahepatic mass-forming cholangiocarcinoma; cHCC-CCA, combined hepatocellular-cholangiocarcinoma; SI, signal intensity.

Table 16. X^2-test result HCC vs. iso-to-high signal intensity group in hepatobiliary phase

	Dark, and iso-to-high SI	Iso-to-high SI	*P*-value
Non-HCC LR-M (n=64)	64	0	0.060
HCC LR-M (n=42)	39	3	

HCC, hepatocellular carcinoma; SI, signal intensity.

D. Histopathologic correlation with hepatobiliary phase signal intensity classification

Histopathologic characteristics of LR-M observations based on hepatobiliary phase signal intensities are summarized in Table 17. In case of iCCA, cHCC-CCA and metastasis, no significant association was found between major histologic differentiation and dark, low and iso-to-high classification. However, in case of HCC, all three observations which showed iso-to-high signal intensity were found to be Edmondson grade 1 and this association was statistically significant (*P*=0.001) (Figure 8). Moreover, HCCs with iso-to-high signal intensity were more significantly associated with pseudoglandular architectural pattern (*P*=0.012). In addition, while not statistically significant, 7 out of 11 scirrhous HCC was found to show low signal intensity (*P*=0.078) (Figure 9).

Table 17. Histopathologic characteristics of malignancies based on HBP signal intensities

Tumor pathology	**Data available**	**Dark**	**Low**	**Iso-to-High**	***P*-value**
HCC (*n*, %)		22 (52)	17 (41)	3 (7)	

Size (mm)	42	35.3 ± 15.9	33.5 ± 18.6	32.2 ± 4.3	0.921
Architectural pattern:	42				
Trabecular		22	16	3	0.476
Pseudoglandular		4	4	3	**0.012**
Compact		1	4	0	0.220
Histologic type	42				
Classical		13	9	3	0.880
Macrotrabecular-massive variant		2	0	0	0.566
Scirrhous variant		4	7	0	0.078
Lymphoepithelioma-like variant		3	0	0	0.397
Sarcomatoid variant		0	1	0	0.476
Major histologic differentiation					
Grade I / II/ III or IV *	42	0 / 16 / 6	0 / 12 / 5	3 / 0 / 0	**0.001**
Intrahepatic mass-forming cholangiocarcinoma, iCCA (*n*, %)		10 (26)	29 (74)	0 (0)	
Size (mm)	39	46.5 ± 27.8	42.2 ± 25.4		0.655
Major histologic differentiation					
Well / moderate / poor / undifferentiated	38	2 / 6 / 1 / 0	5 / 21 / 3 / 0	0 / 0 / 0 / 0	0.429
Combined hepatocellular cholangiocarcinoma, cHCC-CCA (*n*, %)		8 (36)	14 (64)	0 (0)	
Size (mm)	22	42.2 ± 22.5	37.3 ± 12.5		0.583
Major histologic differentiation					
Well / moderate / poor / undifferentiated	22	1 / 5 / 3	1 / 7 / 4 / 1	0 / 0 / 0 / 0	0.892
Metastasis (*n*, %)		2 (67)	1 (33)	0 (0)	
Size (mm)		29.2 ± 16.7	40.0 ± 0		0.691
Major histologic differentiation					
Well / moderate / poor / undifferentiated	3	0 / 1 / 1 / 0	0 / 1 / 0 / 0	0 / 0 / 0 / 0	0.667
Total patients (*n*, %)					

Tumor necrosis (>5%)					
Absent / Present	105	14 / 28	26 / 34	1 / 2	0.694
Tumor necrosis area, %	105	19.0 ± 23.9	10.9 ± 15.1	6.7 ± 7.6	0.090
Capsular formation					
Absent / Partial / Complete	102	22 / 16 / 2	51 / 4 / 4	0 / 2 / 1	0.451
Microvascular invasion					
Absent / Present	102	10 / 30	23 / 36	2 / 1	0.144

*Histologic differentiation of HCC is based on Edmondson grade

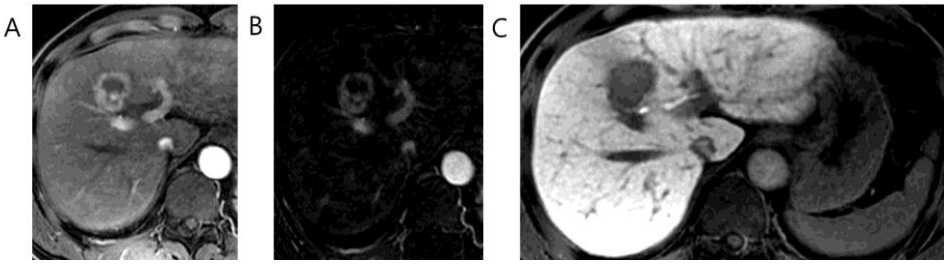

Figure 9. 46 year old male patient with scirrhous HCC. This observation shows rim APHE in (A) late arterial phase, (B) arterial subtraction image and (C) low signal intensity in hepatobiliary phase.

Presence of tumor necrosis (>5%), capsular formation, and microvascular invasion did not significantly differ among dark, low and iso-to-high groups. However, while the difference was nonsignificant, dark group showed larger necrotic percentage followed by low and iso-to-high group (*P*=0.090). In case of scirrhous HCCs, those showing dark signal intensity had significantly higher mean tumor necrosis area compared to those showing low signal intensity (25.0 ± 21.2% vs. 2.5 ± 4.2%, P=0.027).

E. Inter-reader agreement of hepatobiliary phase signal intensity classification

Initially, reviewer 1 and reviewer 2 classified 44 (42%) and 43 (41%) as dark group, 59 (55%) and 60 (57%) as low group, and 3 (3%) and 3 (3%) as iso-to-high group, respectively (Table 18). The inter-reader agreement for hepatobiliary phase signal intensity classification was excellent, with a kappa coefficient of 0.872. Excellent

inter-reader agreement was observed within HCC and within non-HCC malignancies with a kappa coefficient of 0.914 and 0.821, respectively.

Table 18. Inter-reader agreement of HBP signal intensities

	Reviewer 1	Reviewer 2	*K*, kappa	*P*-value
Total patients (n=106)			0.872	<0.001
Dark	44 (42)	43 (41)		
Low	59 (55)	60 (57)		
Iso-to-High	3(3)	3 (3)		
HCC (*n=42*, 40%)			0.914	<0.001
Dark	24 (57)	22 (52)		
Low	15 (36)	17 (41)		
Iso-to-High	3 (7)	3 (7)		
Non-HCC malignancies (*n= 64*, 60%)			0.821	<0.001
Dark	20 (31)	21 (33)		
Low	44 (69)	43 (67)		
Iso-to-High	0 (0)	0 (0)		

A kappa statistic of 0.8-1.0 is considered excellent agreement, 0.6-0.79 good agreement, 0.40-0.59 moderate agreement, 0.2-0.39 fair agreement and 0-0.19 poor agreement.
Abbreviation: HCC, hepatocellular carcinoma

IV. DISCUSSION

1. Diagnostic performance of category adjusted LR-5 using modified criteria

Our results indicate that compared to the diagnostic performance of LR-5 based on LI-RADS v2018, category-readjusted LR-5 after upgrading LR-4 to LR-5 using AF favoring HCC in particular, subthreshold growth as a major feature, extending washout to transitional phase and APHE interpreted using arterial subtraction images can significantly increase sensitivity without reducing specificity for HCC. On the other hand, LR-5 upgraded from LR-4 using AF favoring malignancy in general showed significant decrease in specificity for HCC despite increased sensitivity. With washout being considered when APHE was absent, there were no significant changes in either sensitivity or specificity of LR-5 for HCC.

When categories were adjusted using AFs, upgrading LR-4 to LR-5 with AF favoring malignancy in general was found to significantly decrease the specificity of LR-5 for HCC because most of the LR-4 lesions showed at least one AF favoring malignancy.

This finding is consistent with an explanation given by LI-RADS v2018 [7] where it states that AFs do not show sufficient specificity for HCC. While there have been previous studies demonstrating that AFs favoring malignancy in general show high specificity for HCC [4,45], readjusted LR-5 after applying these features failed to increase specificity. However, aligned with our expectations, LR-5 readjusted after using AF favoring HCC in particular showed no significant reduction in specificity for HCC while increasing the sensitivity for HCC

As for category adjustment after extending APHE to the arterial phase subtraction images, adjusted LR-5 showed increased sensitivity without decreasing the specificity for HCC. This result was consistent with a recent study [36], thereby validating that the use of subtraction image can contribute to the diagnostic accuracy of LR-5 observations. Furthermore, one observation showed rim-like enhancement pattern in arterial phase and was categorized initially as LR-M. However, the subtraction image was helpful in confirming a global enhancement pattern, which with threshold growth and size criterion, recategorized the observation as LR-5 (Figure 10). This observation was later confirmed as HCC, demonstrating that subtraction image can help facilitate categorization of false-positive LR-M observation back to LR-5. Possible explanation is that in case where the tumor center and periphery show enhancement compared to background liver but the tumor center shows slightly weaker enhancement than periphery, this difference in the enhancement degree is eccentuated in late arterial phase and an observation may be mistaken to exhibit rim-like enhancement pattern. However, this difference is less prominant in subtraction image, where both tumor center and periphery show increased intensity when precontrast scan is subtracted from arterial phase, thus showing global enhancement pattern, which the reader can use to correctly categorize an observation as LR-4 or 5.

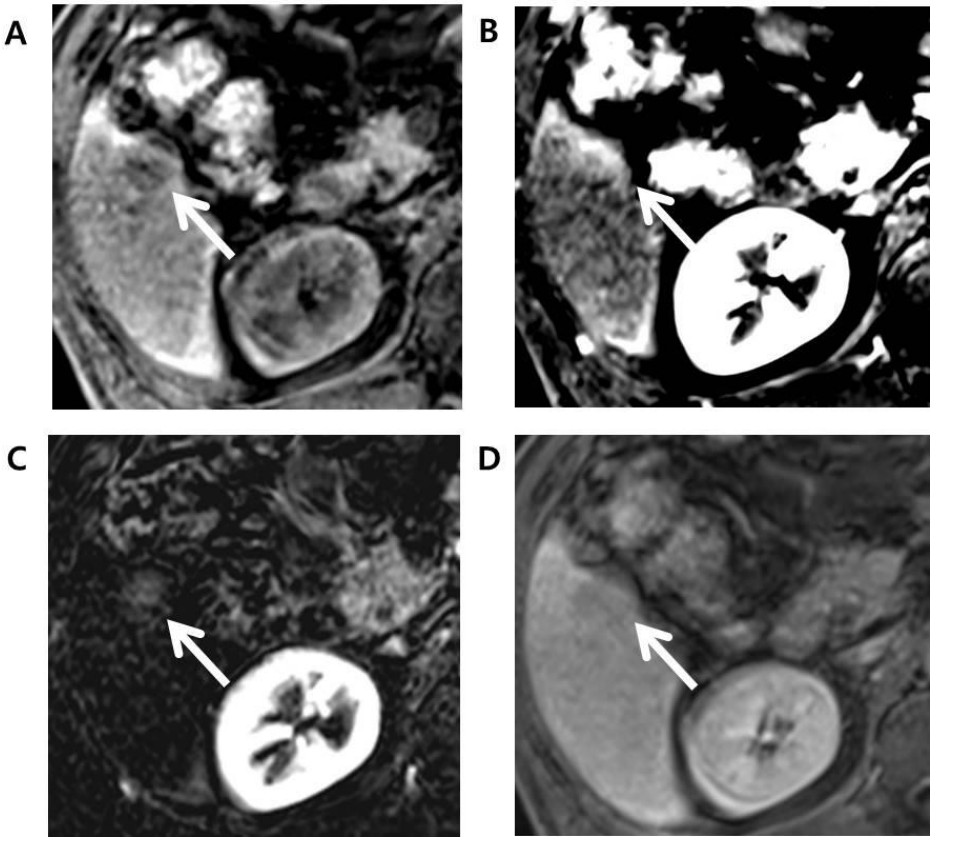

Figure 10. Edmonson grade 1 HCC in 71-year-old male with underlying chronic hepatitis B-viral infection. (A) Axial pre-contrast phase shows a 23mm sized liver mass (arrow) in segment 6 (S6) of the liver. (B) Late arterial phase (AP) shows rim-like arterial hyperenhancement and thus, this observation was categorized as LR-M considering targetoid appearance. (C) Arterial subtraction image, however, shows a global homogeneous enhancement and, with presence of threshold growth, this observation was re-categorized as LR-5. (D) Delayed phase shows hypointensity compared to background liver

LR-5 adjusted while considering no washout when APHE was absent in the artertial phase failed to show any significant change in both sensitivity and specificity for HCC, with the sensitivity for HCC rather showing a slight decrease compared to that of the

original LR-5. While there are debate as to whether washout should be considered at all when APHE is absent, associating washout to APHE allowed LR-5 observations to only downgrade to LR-4 by reducing a major feature. Our result thus indicates that washout should be considered separately from APHE as suggested by the current LI-RADS v2018.

Lastly, we evaluated the diagnostic performance of LR-5 when subthreshold growth is considered a major feature. While only 6.2% of all non-LR-M observations showed category readjustment after applying subthreshold growth as a major feature (i.e. applying the threshold growth criteria of LIRAD v2017), separating subthreshold growth from threshold growth as in LI-RADS v2018 significantly decreased LR-5 sensitivity for HCC, even though no significant reduction was noted for LR-5 specificity. By removing subthreshold growth from major features, some LR-5 observations were recategorized as LR-4 due to the loss of a major feature and this explains for the lower LR-5 sensitivity for HCC.

2. Threshold growth as a major feature in the diagnosis of HCC

The results of our study indicate that when fat-in-nodule replaced threshold growth as a major feature, both LR-5 specificity and sensitivity could be slightly improved although there was no statistical significant difference. When fat-in-nodule was added as an additional major, sensitivity of LR-5 was slightly higher without affecting the specificity. Presence of threshold growth was higher in non-HCC malignancies than in HCC and non-HCC malignancies showing threshold growth were smaller in size compared to those not exhibiting threshold growth.

Intuitively, the presence of threshold growth could be affected by the initial tumor size because the definition of "≥50% increase in diameter in ≤6 months" can be more easily achieved by smaller observations than larger observations. Previous results have also shown that smaller HCCs usually increased in size faster than larger ones, though there are many other factors related to the growth rate of HCC [22,23]. In our study, this trend was more dominant in non-HCC malignancies although it was not statistically

significant. However, when excluding HCCs with size <10 mm, threshold growth was also more frequent in smaller HCC (10-19mm) than larger HCC (≥20mm), although this difference was also not significant. Possible reason for this result could be due to low proportion (n=82, 8.1%) of observations with size <10mm within total observations thus explaining for the low statistical power and also due to the fact that the proportion of small (<10mm) HCC out of total HCCs were less than that of small (<10mm) non HCC malignancies out of total non-HCC malignancies since many of the small HCCs were treated using non-surgical methods such as radiofrequency ablation and transarterial chemoembolization.

Fatty metamorphosis in HCCs have been reported approximately 16-18% of HCC [46], which was consistent with our results (16.1% in HCC) and it was more frequently observed in HCC than in non-HCC malignancies (3.4%). In our study, fat-in-nodule was a more HCC-specific feature than threshold growth and the diagnostic performance of LR-5 for HCC when fat-in-nodule replaced threshold growth as a major feature was comparable to that obtained using the current LI-RADS v2018. In fact, our results showed that when fat-in-nodule replaced threshold growth as a major feature, both LR-5 sensitivity and specificity were non-significantly higher compared to that of original LR-5. Similarly, when fat-in-nodule was added as a major feature, no reduction in LR-5 specificity was noted while the LR-5 sensitivity non-significantly increased by about 0.7%. However, fatty metamorphosis occurs more frequently in early stage HCCs, especially in those with sizes less than 15mm [47]. Thus, the proportion of early HCCs and progressed HCCs in a study population can affect the prevalence of fat-in-nodule.

Regardless, our findings demonstrate the possibility for a comparable LR-5 diagnostic peformance of diagnosing HCC when threshold growth is replaced by a more specific ancillary feature and raises the question as to whether threshold growth has enough scientific evidence to remain as a major feature. One significant limitation of threshold growth is that it cannot be applied in the diagnosis of HCC when previous CT or MRI exam is not available [2]. In our study, 47.7% (438/1,013) of all patients had prior exams in which 32.4% (142/483) patients had hepatic malignancies where in

19.7% (30/142) showed threshold growth. In the case of HCC, 19.3% (119/616) had prior exams wherein 14.2% (17/119) showed threshold growth and this proportion was close to the reported 14.7% in another study where prior exam was available in 66.4% of all patients (N=489 observations) [26]. In their study, Chernyak et al. [26] acknowledged that their study period was too short to include many first-time patients, thus explaining for the relatively larger proportion of patients with prior exams, and stated that this might have inflated the importance of threshold growth. However, the fact that threshold growth affects LI-RADS categorization in only a small proportion of observations is shared in both studies.

Previously, it has been suggested that removing threshold growth from major features will under-categorize aggressive HCCs showing rapid growth which, if left untreated, will be the most harmful to patients [26]. While the histological differentiation of HCC is often heterogeneous, tumor doubling time is reported to correlate significantly with histological differentiation of HCC with more rapid tumor growth reported in poorly differentiated HCCs [24,48,49]. However, our results showed no significant correlation between Edmondson grade of HCC and the presence of threshold growth. Moreover, our results showed that HCCs with threshold growth did not comprise higher Edmondson grade tumors compared to those without threshold growth. Thus, removal of threshold growth from the major features and incorporation into ancillary feactures alongside subthreshold growth may have marginal impact on the exclusion of rapid-growing HCCs. Although threshold growth can be useful in differentiating benign observations such as dysplastic or regenerative nodules and FNH-like nodules from primary hepatic malignancy, it has limited role in differentiating other hepatic malignancies from HCC [4,50,51]. However, considering the fact that based on LI-RADS v2018 algorithm, benign lesions (i.e. LR-1 and LR-2) are often already excluded before assigning a hepatic observation with one of LR-3, -4 and -5 categories, presence of threshold growth, in practice, may have a limited role in the diagnosis of HCC. In our study, two out of 63 (3.2%) dysplastic or regenerative nodules showed threshold growth and were categorized as LR-4 while other nodules were categorized as LR-2 or LR-3.

However, both nodules would still have been categorized as LR-4 via upgrade using threshold growth as an ancillary feature. By keeping threshold growth as an ancillary feature, LR-3 observations can still be upgraded to LR-4 and improve LR-4 diagnostic performance while also preventing non-HCC malignancies from being assigned LR-5 and thus allowing for high LR-5 specificity for HCC.

3. Usefulness of hepatobiliary phase signal intensity in the diagnosis of HCC with atypical imaging features among LR-M observations

In our study, all three LR-M observations that showed iso-to-high signal intensity in hepatobiliary phase were well-differentiated, Edmondson grade 1 HCCs and this association was statistically significant. Furthermore, iso-to-high intensity HCCs were significantly more frequently associated pseudoglandular architectural pattern. On the other hand, nearly 70% (43 out of 61) of LR-M observations that showed low signal intensity in hepatobiliary phase were either cHCC-CCA or iCCA and this association was also significant.

Imaging findings, especially that of hepatobiliary phase signal intensity of tumor may be useful in differentiating HCC with atypical imaging features from non-HCC malignancies among LR-M observations. Importantly, all LR-M observations that showed iso-to-high signal intensity in hepatobiliary phase were HCCs. LR-M observations showing low signal intensity in hepatobiliary phase were more significantly associated with cHCC-CCA or iCCA. As for LR-M observations showing dark signal intensity in hepatobiliary phase, while significant association was found between dark LR-M and HCC, nearly 40% of dark LR-M also comprised of either cHCC-CCA or iCCA, making it a difficult differentiator of HCC from non-HCC malignancies.

In general, tumor signal intensity in hepatobiliary phase is known to decrease significantly during multistep hepatogenesis with worse histologic differentiation [12,52,53]. Consistent with previous studies, the number of iso-to-high signal intensity observations in hepatobiliary phase was highest in well-differentiated HCCs [12,52-54]. Organic

anion-transporting polypeptide 8 (OATP8) expression, which is the most probable uptake transporter of gadoxetic acid, is reported to significantly decrease during multisetep hetatocarcinogenesis due to increased expression of hepatocyte nuclear factor 3β (HNF3β) [53,55], which may explain why iso-to-high signal intensity HCCs were confirmed as well-differentiated HCC. Moreover, iso-to-high intensity HCCs were more significantly associated with higher frequency of pseudoglandular architectural pattern consistent with a previous study [52,56]. Overexpression of OATP8 is thought to contribute to the overproduction of bile because OATP8 can also take up bile acid component, causing pseudoglandular proliferation with bile plugs and secondary dilatation of bile canaliculi [57].

Likewise, significant association between cHCC-CCA or iCCA and low signal intensity in hepatobiliary is consistent with previous studies [58-60]. Such low signal intensity in hepatobiliary phase is thought to relate to the presence of abundant stromal fibrosis in iCCA and cholangiocarcinoma component of cHCC-CCA, which causes extracellular accumulation of contrast agent through large interstitial spaces [59,61].

Similarly, scirrhous HCC is known to exhibit fibrous tumor stroma generated by cancer-associated fibroblasts and peritumoral myofibroblasts through cross-talk with HCC cells [62]. In our study, more than half (58%) of scirrhous HCCs showed low signal intensity consistent with previous studies [63,64]. Similar to iCCA and cHCC-CCA, scirrhous HCCs that did not show low signal intensity in hepatobiliary phase showed dark signal intensities. Previously, studies on iCCA have reported heterogeneous tumor enhancement pattern in hepatobiliary phase to be attributed to amount and density of fibrous component [65], timing of hepatobiliary phase and predominance of necrosis over fibrosis [66]. Importantly, however, combined together, iCCA, cHCC-CCA and scirrhous HCC comprised 82% of all low signal intensity LR-M observations.

Admittedly, the number of LR-M showing iso-to-high signal intensity in our study is small despite statistical significance. However, when LR-M designation was first introduced to cover non-HCC malignancies in LI-RADS, the primary goal was to preserve high specificity of LR-5 without losing the sensitivity for diagnosing all

hepatic malignancies. In our study, patient at high risk of HCC of either cirrhosis or chronic hepatitis B-viral infection with BCLC stage 0/A and mainly Child-Pugh class A were included, all of whom if the tumor is diagnosed properly as HCC can be potential candidate for liver transplantation. Likewise, the result of our study suggests that in patients with LR-M observations exhibiting low signal intensity in hepatobiliary phase, imaging prediction of tumor containing fibrous stroma such as iCCA, cHCC-CCA and scirrhous HCC are high and may influence the need and urgency of biopsy. These tumors are generally associated with poor overall survival and prognosis [29,67] and in case of iCCA and cHCC-CCA, if diagnosed, the patient is not suitable for transplantation in order to allocate organs for more appropriate disease [31,32,68].

4. Summary of above investigations

In this study, we evaluated possible methods of increasing LR-5 specificity for HCC. Initially, we verified several strategies of increasing LR-5 sensitivity without losing LR-5 specificity as previously suggested by independent studies using our study patients and found that upgrading LR-4 to LR-5 using AF favoring HCC in particular, using subthreshold growth as a major feature, extending washout to transitional phase, and interpreting APHE using arterial subtraction can improve diagnostic performance of LR-5 compared to that of LI-RADS v2018. We then evaluated whether threshold growth should continue to remain as a major feature considering its arbitrary definition and absence of pathophysiologic basis and found that threshold growth is more specific to non-HCC malignancy than HCC and when it is replaced by a more-HCC specific AF such as fat-in-nodule, comparable LR-5 sensitivity and specificity can still be obtained. Lastly, we speculated that another way of improving LR-5 specificity for HCC is to salvage HCC with atypical features from LR-M by correctly diagnosing them as LR-5. Using HBP signal intensity of tumor, we found that HBP iso-to-high signal intensity observations are all well-differentiated HCC. Thus, we hope that by applying the above strategies, considering threshold growth as ancillary feature rather than a major feature and using HBP signal intensity of LR-M observations, LR-5 diagnostic performance for

HCC may be improved significantly from that of LI-RADS v2018.

V. LIMITATIONS

There are some limitations to this study. First, there may have been a selection bias due to its retrospective design and inclusion of patients with pathologically confirmed hepatic observations. While only surgically resected hepatic malignancies were included, pathologic confirmation was necessary to accurately evaluate the prevalence of major and ancillary features as well as to perform imaging-histologic correlation and because non-HCC malignancies such as cHCC-CCA can be misinterpreted as HCC based on imaging finding alone. Secondly, image analysis was performed by two radiologists in consensus and thus, no interobserver agreement was determined for the LI-RADS categories. Thirdly, more than half of all included observations did not have prior exams due to tertiary hospital setting and this may have underestimated the importance of threshold growth. Lastly, all patients underwent gadoxetate disodium MRI which is known to show more ghosting artifacts in arterial phase known as transient severe motion artifact than extracellular agent (ECA) based MRI, but we did not encounter difficulty during image analysis as patients underwent MRI re-examination when transient severe motion artifact impeded image analysis. Moreover, there were some minor modification to imaging protocols during the time period. However, these modifications were not significant enough to influence interpretation.

VI. CONCLUSION

Our results suggest that upgrading LR-4 to LR-5 using AF favoring HCC in particular, using subthreshold growth as a major feature, extending washout to transitional phase, and interpreting APHE using arterial subtraction image significantly increased the sensitivity of LR-5 for HCC without significantly reducing the specificity.

In case of threshold growth, threshold growth can occur both in HCC and non-HCC malignancies but is more common among non-HCC malignancies and can be affected

by the initial tumor size. Radiologists should be precautious when upgrading LR-4 observation to LR-5 using threshold growth as the sole determining factor. When threshold growth is considered an ancillary feature and major feature is either replaced or added by a different ancillary feature more specific to HCC, no significant reduction in LR-5 diagnostic performance was observed compared to LI-RADS v2018.

In addition, LR-M observation showing iso-to-high signal intensity in hepatobiliary phase has high potential to be well-differentiated HCC while LR-M observations showing low signal intensity in hepatobiliary phase has high potential to be tumor with fibrous stroma such as iCCA, cHCC-CCA, or scirrhous HCC. Thus, classification of LR-M observations based on hepatobiliary phase signal intensity may be a helpful in differentiating HCC with atypical imaging features from non-HCC malignancies.

REFERENCES

1. Bruix J, Sherman M. Management of hepatocellular carcinoma: an update. Hepatology 2011;53:1020-2.
2. Kim YY, Choi JY, Sirlin CB, An C, Kim MJ. Pitfalls and problems to be solved in the diagnostic CT/MRI Liver Imaging Reporting and Data System (LI-RADS). Eur Radiol 2019;29:1124-32.
3. Elsayes KM, Kielar AZ, Chernyak V, Morshid A, Furlan A, Masch WR, et al. LI-RADS: a conceptual and historical review from its beginning to its recent integration into AASLD clinical practice guidance. J Hepatocell Carcinoma 2019;6:49-69.
4. Cerny M, Bergeron C, Billiard JS, Murphy-Lavallee J, Olivie D, Berube J, et al. LI-RADS for MR Imaging Diagnosis of Hepatocellular Carcinoma: Performance of Major and Ancillary Features. Radiology 2018;288:118-28.
5. Kim YY, Kim MJ, Kim EH, Roh YH, An C. Hepatocellular Carcinoma versus Other Hepatic Malignancy in Cirrhosis: Performance of LI-RADS Version 2018. Radiology 2019;291:72-80.
6. Lee SM, Lee JM, Ahn SJ, Kang HJ, Yang HK, Yoon JH. LI-RADS Version 2017 versus Version 2018: Diagnosis of Hepatocellular Carcinoma on Gadoxetate Disodium-enhanced MRI. Radiology 2019;292:655-63.
7. Radiology ACo. CT/MRI LI-RADS v2018 core. Liver Imaging Reporting and Data System. Available at: https://www.acr.org/-/media/ACR/Files/RADS/LI-RADS/LI-RADS-2018-Core.pdf?la=en
8. Marrero JA, Kulik LM, Sirlin CB, Zhu AX, Finn RS, Abecassis MM, et al. Diagnosis, Staging, and Management of Hepatocellular Carcinoma: 2018 Practice Guidance by the American Association for the Study of Liver Diseases. Hepatology 2018;68:723-50.
9. Rosenkrantz AB, Campbell N, Wehrli N, Triolo MJ, Kim S. New OPTN/UNOS classification system for nodules in cirrhotic livers detected with MR imaging: effect on hepatocellular carcinoma detection and transplantation allocation. Radiology 2015;274:426-33.
10. Lee S, Kim SS, Bae H, Shin J, Yoon JK, Kim MJ. Application of Liver Imaging Reporting and Data System version 2018 ancillary features to upgrade from LR-4 to LR-5 on gadoxetic acid-enhanced MRI. Eur Radiol 2021;31:855-63.
11. Efremidis SC, Hytiroglou P. The multistep process of hepatocarcinogenesis in cirrhosis with imaging correlation. Eur Radiol 2002;12:753-64.
12. Choi JW, Lee JM, Kim SJ, Yoon JH, Baek JH, Han JK, et al. Hepatocellular carcinoma: imaging patterns on gadoxetic acid-enhanced MR Images and their value as an imaging biomarker. Radiology

2013;267:776-86.
13. Choi JY, Lee JM, Sirlin CB. CT and MR imaging diagnosis and staging of hepatocellular carcinoma: part II. Extracellular agents, hepatobiliary agents, and ancillary imaging features. Radiology 2014;273:30-50.
14. Matsui O, Kobayashi S, Sanada J, Kouda W, Ryu Y, Kozaka K, et al. Hepatocelluar nodules in liver cirrhosis: hemodynamic evaluation (angiography-assisted CT) with special reference to multi-step hepatocarcinogenesis. Abdom Imaging 2011;36:264-72.
15. Forner A, Vilana R, Ayuso C, Bianchi L, Sole M, Ayuso JR, et al. Diagnosis of hepatic nodules 20 mm or smaller in cirrhosis: Prospective validation of the noninvasive diagnostic criteria for hepatocellular carcinoma. Hepatology 2008;47:97-104.
16. Kim TK, Lee KH, Jang HJ, Haider MA, Jacks LM, Menezes RJ, et al. Analysis of gadobenate dimeglumine-enhanced MR findings for characterizing small (1-2-cm) hepatic nodules in patients at high risk for hepatocellular carcinoma. Radiology 2011;259:730-8.
17. Ishigami K, Yoshimitsu K, Nishihara Y, Irie H, Asayama Y, Tajima T, et al. Hepatocellular carcinoma with a pseudocapsule on gadolinium-enhanced MR images: correlation with histopathologic findings. Radiology 2009;250:435-43.
18. Lim JH, Choi D, Park CK, Lee WJ, Lim HK. Encapsulated hepatocellular carcinoma: CT-pathologic correlations. Eur Radiol 2006;16:2326-33.
19. 2018 Korean Liver Cancer Association-National Cancer Center Korea Practice Guidelines for the Management of Hepatocellular Carcinoma. Gut Liver 2019;13:227-99.
20. Omata M, Cheng AL, Kokudo N, Kudo M, Lee JM, Jia J, et al. Asia-Pacific clinical practice guidelines on the management of hepatocellular carcinoma: a 2017 update. Hepatol Int 2017;11:317-70.
21. EASL Clinical Practice Guidelines: Management of hepatocellular carcinoma. J Hepatol 2018;69:182-236.
22. Kim JK, Kim HD, Jun MJ, Yun SC, Shim JH, Lee HC, et al. Tumor Volume Doubling Time as a Dynamic Prognostic Marker for Patients with Hepatocellular Carcinoma. Dig Dis Sci 2017;62:2923-31.
23. An C, Choi YA, Choi D, Paik YH, Ahn SH, Kim MJ, et al. Growth rate of early-stage hepatocellular carcinoma in patients with chronic liver disease. Clin Mol Hepatol 2015;21:279-86.
24. Shingaki N, Tamai H, Mori Y, Moribata K, Enomoto S, Deguchi H, et al. Serological and histological indices of hepatocellular carcinoma and tumor volume doubling time. Mol Clin Oncol 2013;1:977-81.
25. De Rose AM, Cucchetti A, Clemente G, Ardito F, Giovannini I, Ercolani G, et al. Prognostic significance of tumor doubling time in mass-forming type cholangiocarcinoma. J Gastrointest Surg

2013;17:739-47.
26. Chernyak V, Kobi M, Flusberg M, Fruitman KC, Sirlin CB. Effect of threshold growth as a major feature on LI-RADS categorization. Abdom Radiol (NY) 2017;42:2089-100.
27. Tang A, Bashir MR, Corwin MT, Cruite I, Dietrich CF, Do RKG, et al. Evidence Supporting LI-RADS Major Features for CT- and MR Imaging-based Diagnosis of Hepatocellular Carcinoma: A Systematic Review. Radiology 2018;286:29-48.
28. Ren AH, Zhao PF, Yang DW, Du JB, Wang ZC, Yang ZH. Diagnostic performance of MR for hepatocellular carcinoma based on LI-RADS v2018, compared with v2017. J Magn Reson Imaging 2019;50:746-55.
29. Choi SH, Lee SS, Park SH, Kim KM, Yu E, Park Y, et al. LI-RADS Classification and Prognosis of Primary Liver Cancers at Gadoxetic Acid-enhanced MRI. Radiology 2019;290:388-97.
30. Chernyak V, Fowler KJ, Kamaya A, Kielar AZ, Elsayes KM, Bashir MR, et al. Liver Imaging Reporting and Data System (LI-RADS) Version 2018: Imaging of Hepatocellular Carcinoma in At-Risk Patients. Radiology 2018;289:816-30.
31. Magistri P, Tarantino G, Serra V, Guidetti C, Ballarin R, Di Benedetto F. Liver transplantation and combined hepatocellular-cholangiocarcinoma: Feasibility and outcomes. Dig Liver Dis 2017;49:467-70.
32. Sapisochin G, Javle M, Lerut J, Ohtsuka M, Ghobrial M, Hibi T, et al. Liver Transplantation for Cholangiocarcinoma and Mixed Hepatocellular Cholangiocarcinoma: Working Group Report From the ILTS Transplant Oncology Consensus Conference. Transplantation 2020;104:1125-30.
33. Llovet JM, Brú C, Bruix J. Prognosis of hepatocellular carcinoma: the BCLC staging classification. Semin Liver Dis 1999;19:329-38.
34. Vogel A, Cervantes A, Chau I, Daniele B, Llovet JM, Meyer T, et al. Hepatocellular carcinoma: ESMO Clinical Practice Guidelines for diagnosis, treatment and follow-up. Ann Oncol 2018;29:iv238-iv55.
35. Mazzaferro V, Regalia E, Doci R, Andreola S, Pulvirenti A, Bozzetti F, et al. Liver transplantation for the treatment of small hepatocellular carcinomas in patients with cirrhosis. N Engl J Med 1996;334:693-9.
36. Lee HS, Kim MJ, An C. How to utilize LR-M features of the LI-RADS to improve the diagnosis of combined hepatocellular-cholangiocarcinoma on gadoxetate-enhanced MRI? Eur Radiol 2019;29:2408-16.
37. Kim MY, Joo I, Kang HJ, Bae JS, Jeon SK, Lee JM. LI-RADS M (LR-M) criteria and reporting algorithm of v2018: diagnostic values in the assessment of primary liver cancers on gadoxetic acid-enhanced MRI. Abdom Radiol (NY) 2020;45:2440-8.
38. Kim SS, Lee S, Choi JY, Lim JS, Park MS, Kim MJ. Diagnostic

performance of the LR-M criteria and spectrum of LI-RADS imaging features among primary hepatic carcinomas. Abdom Radiol (NY) 2020;45:3743-54.
39. Joo I, Lee JM, Yoon JH. Imaging Diagnosis of Intrahepatic and Perihilar Cholangiocarcinoma: Recent Advances and Challenges. Radiology 2018;288:7-13.
40. Batts KP, Ludwig J. Chronic hepatitis. An update on terminology and reporting. Am J Surg Pathol 1995;19:1409-17.
41. Seo N, Chung YE, Park YN, Kim E, Hwang J, Kim MJ. Liver fibrosis: stretched exponential model outperforms mono-exponential and bi-exponential models of diffusion-weighted MRI. Eur Radiol 2018;28:2812-22.
42. Edmondson HA, Steiner PE. Primary carcinoma of the liver: a study of 100 cases among 48,900 necropsies. Cancer 1954;7:462-503.
43. Lee S, Kim MJ, Kim SS, Shin H, Kim DY, Choi JY, et al. Retrospective comparison of EASL 2018 and LI-RADS 2018 for the noninvasive diagnosis of hepatocellular carcinoma using magnetic resonance imaging. Hepatol Int 2020;14:70-9.
44. Koh J, Chung YE, Nahm JH, Kim HY, Kim KS, Park YN, et al. Intrahepatic mass-forming cholangiocarcinoma: prognostic value of preoperative gadoxetic acid-enhanced MRI. Eur Radiol 2016;26:407-16.
45. Alhasan A, Cerny M, Olivie D, Billiard JS, Bergeron C, Brown K, et al. LI-RADS for CT diagnosis of hepatocellular carcinoma: performance of major and ancillary features. Abdom Radiol (NY) 2019;44:517-28.
46. Cerny M, Chernyak V, Olivie D, Billiard JS, Murphy-Lavallee J, Kielar AZ, et al. LI-RADS Version 2018 Ancillary Features at MRI. Radiographics 2018;38:1973-2001.
47. Cho ES, Choi JY. MRI features of hepatocellular carcinoma related to biologic behavior. Korean J Radiol 2015;16:449-64.
48. Cucchetti A, Vivarelli M, Piscaglia F, Nardo B, Montalti R, Grazi GL, et al. Tumor doubling time predicts recurrence after surgery and describes the histological pattern of hepatocellular carcinoma on cirrhosis. J Hepatol 2005;43:310-6.
49. Ebara M, Hatano R, Fukuda H, Yoshikawa M, Sugiura N, Saisho H. Natural course of small hepatocellular carcinoma with underlying cirrhosis. A study of 30 patients. Hepatogastroenterology 1998;45 Suppl 3:1214-20.
50. An C, Rakhmonova G, Choi JY, Kim MJ. Liver imaging reporting and data system (LI-RADS) version 2014: understanding and application of the diagnostic algorithm. Clin Mol Hepatol 2016;22:296-307.
51. Borzio M, Fargion S, Borzio F, Fracanzani AL, Croce AM, Stroffolini T, et al. Impact of large regenerative, low grade and high grade dysplastic

nodules in hepatocellular carcinoma development. J Hepatol 2003;39:208-14.
52. Kitao A, Zen Y, Matsui O, Gabata T, Kobayashi S, Koda W, et al. Hepatocellular carcinoma: signal intensity at gadoxetic acid-enhanced MR Imaging--correlation with molecular transporters and histopathologic features. Radiology 2010;256:817-26.
53. Kitao A, Matsui O, Yoneda N, Kozaka K, Shinmura R, Koda W, et al. The uptake transporter OATP8 expression decreases during multistep hepatocarcinogenesis: correlation with gadoxetic acid enhanced MR imaging. Eur Radiol 2011;21:2056-66.
54. Huppertz A, Haraida S, Kraus A, Zech CJ, Scheidler J, Breuer J, et al. Enhancement of focal liver lesions at gadoxetic acid-enhanced MR imaging: correlation with histopathologic findings and spiral CT--initial observations. Radiology 2005;234:468-78.
55. Vavricka SR, Jung D, Fried M, Grützner U, Meier PJ, Kullak-Ublick GA. The human organic anion transporting polypeptide 8 (SLCO1B3) gene is transcriptionally repressed by hepatocyte nuclear factor 3beta in hepatocellular carcinoma. J Hepatol 2004;40:212-8.
56. Tsuboyama T, Onishi H, Kim T, Akita H, Hori M, Tatsumi M, et al. Hepatocellular carcinoma: hepatocyte-selective enhancement at gadoxetic acid-enhanced MR imaging--correlation with expression of sinusoidal and canalicular transporters and bile accumulation. Radiology 2010;255:824-33.
57. Kondo Y, Nakajima T. Pseudoglandular hepatocellular carcinoma. A morphogenetic study. Cancer 1987;60:1032-7.
58. Kim SH, Lee CH, Kim BH, Kim WB, Yeom SK, Kim KA, et al. Typical and Atypical Imaging Findings of Intrahepatic Cholangiocarcinoma Using Gadolinium Ethoxybenzyl Diethylenetriamine Pentaacetic Acid–Enhanced Magnetic Resonance Imaging. 2012;36:704-9.
59. Jeong HT, Kim M-J, Chung YE, Choi JY, Park YN, Kim KW. Gadoxetate Disodium–Enhanced MRI of Mass-Forming Intrahepatic Cholangiocarcinomas: Imaging-Histologic Correlation. American Journal of Roentgenology 2013;201:W603-W11.
60. Jeon TY, Kim SH, Lee WJ, Lim HK. The value of gadobenate dimeglumine–enhanced hepatobiliary-phase MR imaging for the differentiation of scirrhous hepatocellular carcinoma and cholangiocarcinoma with or without hepatocellular carcinoma. Abdom Imaging 2010;35:337.
61. Gabata T, Matsui O, Kadoya M. Delayed MR imaging of the liver: correlation of delayed enhancement of hepatic tumors and pathologic appearance. Abdom Imaging 1998;23:309.
62. Rhee H, Kim HY, Choi JH, Woo HG, Yoo JE, Nahm JH, et al. Keratin

19 Expression in Hepatocellular Carcinoma Is Regulated by Fibroblast-Derived HGF via a MET-ERK1/2-AP1 and SP1 Axis. Cancer Res 2018;78:1619-31.

63. Kim SS, Ah Hwang J, Cheol Shin H, Auck Hong S, Shick Jou S, Hee Lee W, et al. Synchronous Occurrence of Classic and Scirrhous Hepatocellular Carcinomas: A Case Report. 2018;15:e65346.
64. Park MJ, Kim YK, Park HJ, Hwang J, Lee WJ. Scirrhous hepatocellular carcinoma on gadoxetic acid-enhanced magnetic resonance imaging and diffusion-weighted imaging: emphasis on the differentiation of intrahepatic cholangiocarcinoma. J Comput Assist Tomogr 2013;37:872-81.
65. Feng ST, Wu L, Cai H, Chan T, Luo Y, Dong Z, et al. Cholangiocarcinoma: spectrum of appearances on Gd-EOB-DTPA-enhanced MR imaging and the effect of biliary function on signal intensity. BMC Cancer 2015;15:38.
66. Chong YS, Kim YK, Lee MW, Kim SH, Lee WJ, Rhim HC, et al. Differentiating mass-forming intrahepatic cholangiocarcinoma from atypical hepatocellular carcinoma using gadoxetic acid-enhanced MRI. Clin Radiol 2012;67:766-73.
67. Lee K, Lee KB, Jung HY, Yi NJ, Lee KW, Suh KS, et al. The correlation between poor prognosis and increased yes-associated protein 1 expression in keratin 19 expressing hepatocellular carcinomas and cholangiocarcinomas. BMC Cancer 2017;17:441.
68. Panjala C, Senecal DL, Bridges MD, Kim GP, Nakhleh RE, Nguyen JH, et al. The diagnostic conundrum and liver transplantation outcome for combined hepatocellular-cholangiocarcinoma. Am J Transplant 2010;10:1263-7.

ABSTRACT(IN KOREAN)

간 영상 보고 및 데이터 시스템(이하 LI-RADS, 2018년 개정판)에 따른 LR-5 카테고리의 간세포암 진단성적 향상을 위한 다양한 접근 방식에 대한 고찰

<지도교수 정용은>

연세대학교 대학원 의학과

박재현

간 영상 보고 및 데이터 시스템 (이하 LIRADS)은 간세포암의 비침습적인 진단을 위해 널리 사용되고 있다. 본 연구에서는 다음과 같은 연구 주제들에 대하여 조사하였다: (1)) LR-5 카테고리의 간세포암 특이도 (specificity)를 감소시키지 않고서 민감도 (sensitivity)를 올릴 수 있는 방법들을 살펴보았고, (2) 간세포암 진단의 주요소견 중 하나인 한계성장 (threshold growth)이 주요소견으로 반드시 적용되어야 할 지의 여부를 살펴보았으며, (3) 병변이 보이는 간담도기 신호강도가 LR-M 카테고리 병변들 중 간세포암을 진단하는데 유용한 소견으로 적용 가능한지 여부를 살펴보았다. 본 연구에서는 간내 종양으로 치료를 받은 과거력이 없는 환자이면서 가도세틱산 (gadoxetic acid) 조영 증강 자기공명영상 검사 및 국소 간내 병변에 대하여 수술적 치료를 받은 환자들을 후향적으로 분석하였다.

LR-5 카테고리의 진단성적을 향상시킬 수 있는 방법들을 조사하기 위해 국소 간내 병변들을 2018년도 간 영상 보고 및 데이터 시스템 (LI-RADS)에 따라 분류를 하였으며, 최종 LR 카테고리는 보조영상소견

(ancillary feature)의 유무에 따라 LR-4를 LR-5로 상승시키거나, 동맥기 조영증강 또는 과혈관성 여부를 동맥기 감산 (subtraction) 영상에서까지 해석을 하거나, 문맥기 조영감소 또는 씻김이 없는 경우 동맥기 조영증강 또는 과혈관성이 없다고 보거나, 문맥기 조영감소 또는 씻김 여부를 지연기에서까지 해석하거나, 역치이하 성장 (subthreshold growth)을 간세포암의 주요소견으로 해석을 하여 변화를 주었다. 그 결과, 간세포암 특이 보조영상소견을 사용하여 LR-4를 LR-5으로 올린 경우, 역치이하 성장을 주요소견으로 해석한 경우, 문맥기 조영감소 및 씻김을 지연기에서까지 해석한 경우 및 조영증강 또는 과혈관성을 동맥기 감산 영상에서까지 해석한 경우 LR-5의 sensitivity가 유의미하게 증가하면서 (P<0.001), 특이도는 유의미한 변화를 보이지 않는 것을 확인하였다 (Ps>0.05).

한계성장 (threshold growh)이 LR-5의 높은 진단성적을 유지하기 위해 계속 주요소견으로 남아야 하는지 여부를 알기 위하여 간 영상 보고 및 데이터 시스템에서 정의하는 주요소견과 보조영상소견들의 빈도를 간세포암군과 간세포암을 제외한 악성 간내 종양군에서 조사하였다. 간세포암에서 더욱 높은 빈도를 보인 보조영상소견들은 한계성장을 치환하거나 추가적인 주요소견으로 사용되었으며 이러한 조건에서의 LR-5의 진단성적은 2018년도 간 영상 보고 및 데이터 시스템에 따른 LR-5 진단성적과 비교하였다. 동맥기 조영증강, 문맥기 씻김 및 피막모양 소견들은 간세포암을 제외한 간내 악성 종양에서보다 간세포암에서 더욱 높은 빈도를 보였으나, 한계성장은 간세포암을 제외한 간내 악성 종양에서 더욱 높은 빈도를 보였다 (P<0.001). 한계성장을 보인 간세포암을 제외한 간내 악성 종양의 평균 크기는 한계성장을 보이지 않았던 군에 비해 작았으며 (22.2mm vs. 42.9mm, P=0.040), 이러한 경향은 간세포암에서도 관찰되었으나 이는 통계학적으로 유의미하지 않았다 (26.8mm vs. 33.1mm, P=0.184). 종양 내 지방 (fat in nodule) 소견은 간세포암을 제외한 간내 악성 종양보다 간세포암에서 더욱 높은 빈도로 관찰되었다 (P=0.027). 종양 내 지방 (fat in nodule)이 한계성장을 치환하여 주요소견이었을 시 LR-5의 민감도는 73.2%에서 73.9%로 (P=0.289), 특이도는 98.2%에서 98.5%로 유의미한

변화를 보이지 않았다 (*P*>0.999).

종양의 간담도기 신호강도가 비특이적 영상소견을 지닌 간세포암을 간세포암을 제외한 간내 악성종양으로부터 감별하는 데 유용하게 사용될 수 있는지를 확인하기 위해, LR-M 카테고리 병변들의 간담도기 신호강도를 매우 저신호, 저신호, 동신호 및 고신호 세 가지 그룹으로 분류를 하였다. 종양 내 50%이상의 면적의 신호강도가 비장의 평균 신호 강도보다 낮은 경우, 매우 저신호 강도로 분류하였고, 종양 내 50%이상의 면적의 신호강도가 비장의 평균 신호강도보다 높으나 정상 간 조직의 신호강도보다 낮은 경우 저신호 강도로 분류하였으며, 종양 내 정상 간 조직의 신호강도와 대등하거나 높은 조직이 부분적으로나마 관찰된 경우 동신호 및 고신호 강도로 분류하였다. 임상병리 인자들과 영상-조직학적 소견들 간의 연관성을 분석하였다. 총 106개의 LR-M 병변들 중, 42개 (42%)가 매우 저신호, 61개 (58%)가 저신호 그리고 3개 (3%)가 동신호 또는 고신호 강도로 분류가 되었다. 동신호 또는 고신호 강도를 보였던 3개 병변들 모두 간세포암이었으며 (*P*=0.060) 모두 병리 소견상 좋은 분화도 (Edmondon grade 1)를 보였다 (*P*=0.001). 저신호 강도를 보였던 61개의 LR-M 병변들 중 43개(71%)는 간내 담관암 (intrahepatic cholangiocarcinoma) 또는 담관상피암종의 중간형 (combined hepatocellular-cholangiocarcinoma)으로 확인되었다 (*P*=0.002). 종양의 간담도기 신호강도의 평가자간 합치도 (inter-reader agreement)는 0.872로 높았으며 카파 통계도 (kappa coefficient)도 0.872로 측정되었다.

결론적으로, LR-5의 민감도는 특이도의 손실 없이 보조영상소견을 통해 LR-4를 LR-5으로 상승시킨 경우, 역치이하 성장을 주요소견으로 해석한 경우, 문맥기 조영감소 및 씻김을 지연기에서까지 해석한 경우, 동맥기 조영증강 또는 과혈관성을 동맥기 감산 영상에서까지 해석한 경우 향상되었다. 또한 한계성장 소견은 간세포암에 비특이적인 소견이며, 오히려 간세포암을 제외한 악성 간내 종양에 더 높은 빈도로 관찰되었다. 상기 결과들을 미룰 때, 한계성장을 간세포암에 특이적인 보조영상소견으로 치환시킬 때 LR-5의 비슷한 진단성적을 도출해낼 수 있는 것을 확인할 수 있었다. 마지막으로 간담도기에서 동신호 또는

고신호 강도를 보인 LR-M 병변은 간세포암일 가능성이 높으며, 저신호 강도를 보인 LR-M 병변은 간내 담관암 (intrahepatic cholangiocarcinoma) 또는 담관상피암종의 중간형 (combined hepatocellular-cholangiocarcinoma) 과 같은 섬유기질을 포함하는 간내 악성 종양일 가능성이 높은 것을 확인하였다. 간담도기 때 종양의 신호강도로 LR-M 병변을 분류하는 방식이 간세포암을 제외한 간내 악성 종양으로부터 간세포암을 감별하는데 도움을 줄 수 있을 것으로 사료된다.

핵심되는 말 : 간내 신생물, 자기공명영상, 간, 진단, 감별

PUBLICATION LIST

1. Park JH, Chung YE, Seo N, Choi JY, Park MS, Kim MJ. Gadoxetic acid-enhanced MRI of hepatocellular carcinoma: Diagnostic performance of category-adjusted LR-5 using modified criteria. PLoS One 2020;15:e0242344.